UHASSELT
KNOWLEDGE IN ACTION

Maastricht University

Faculteit Geneeskunde en Levenswetenschappen
School voor Levenswetenschappen

master in de biomedische wetenschappen

Masterthesis

Functional characterization of placental mitochondria from women exposed to environmental stressors

Stijn Vos

Scriptie ingediend tot het behalen van de graad van master in de biomedische wetenschappen, afstudeerrichting milieu en gezondheid

PROMOTOR :
Prof. dr. Tim NAWROT

COPROMOTOR :
dr. Bram JANSSEN

2018
2019

De transnationale Universiteit Limburg is een uniek samenwerkingsverband van twee universiteiten in twee landen: de Universiteit Hasselt en Maastricht University.

UHASSELT
KNOWLEDGE IN ACTION

www.uhasselt.be
Universiteit Hasselt
Campus Hasselt:
Martelarenlaan 42 | 3500 Hasselt
Campus Diepenbeek:
Agoralaan Gebouw D | 3590 Diepenbeek

UHASSELT
KNOWLEDGE IN ACTION

Maastricht University

Faculteit Geneeskunde en Levenswetenschappen

School voor Levenswetenschappen

master in de biomedische wetenschappen

Masterthesis

Functional characterization of placental mitochondria from women exposed to environmental stressors

Stijn Vos

Scriptie ingediend tot het behalen van de graad van master in de biomedische wetenschappen, afstudeerrichting milieu en gezondheid

PROMOTOR :
Prof. dr. Tim NAWROT

COPROMOTOR :
dr. Bram JANSSEN

Acknowledgements

As I finish this master thesis project, I would like to reflect on the eight-month journey that lead me here and thank the people that made the completion of this master thesis possible.

First, I would like to thank my supervisor and co-promotor dr. Bram Janssen for his continued support, personal coaching and mentorship. Thanks to his patience, knowledge and willingness to help, I was able to learn a broad range of new skills and knowledge. Not only were these elements essential in the successful completion of this internship, but I am confident they will also help me in my future pursuits in life. I would also like to thank my promotor, Prof. dr. Tim Nawrot, for his support and helpful suggestions during the course of this research project, and for the opportunity to use some state-of-the-art research technologies.

There are several additional people from the environmental epidemiology research group that have contributed significantly to this project. Therefore, I would like to thank dr. Hannelore Bové and Eva Bongaerts for their time and help with the parts of this project that made use of confocal microscopy, as well as for providing us with the microscopy image that was used for the results section of this thesis. For showing me the ins and outs of the recruitment for the ENVIR*ON*AGE birth cohort at the East-Limburg Hospital in Genk, I would like to thank Hanne Sleurs, Riccardo Carollo and Kristof Neven. For his help with the execution and interpretation of the mtDNA content assays, I would like to thank dr. Dries Martens. I would also like to thank dr. Bianca Cox for her contributions to the statistical analysis of the DNA methylation data. Additionally, I am very grateful for the positive working environment and support from my fellow students at the Centre for Environmental Sciences (CMK).

Finally, I would like to express my gratitude to my closest family members and friends, that have helped me during the most challenging and stressful periods I have faced throughout my education. Without their continued support and belief, I would have never made it this far.

Contents

Abbreviations

Acetyl CoA	Acetyl Coenzyme A
ADP	Adenosine diphosphate
AP	Air Pollution
ATP	Adenosine triphosphate
BC	Black carbon
BMI	Body mass index
Ca^{2+}	Calcium
ENVIR*ON*AGE	ENVIRonmental influence *ON* AGEing
ETC	Electron transport chain
FAD	Flavin adenine dinucleotide (oxidized form)
$FADH_2$	Flavin adenine dinucleotide (reduced form)
GPx	Glutathione peroxidase
GSH	Glutathione
GSSG	Glutathione disulfide
H_2O_2	Hydrogen peroxide
MeDIP	Methylated DNA immunoprecipitation
mtDNA	Mitochondrial DNA
mtDNMT1	Mitochondrial-localized DNA methyltransferase 1
NAD+	Nicotinamide adenine dinucleotide (oxidized form)
NADH	Nicotinamide adenine dinucleotide (reduced form)
O_2^{*-}	Superoxide
OH^*	Hydroxyl radical
OXPHOS	Oxidative phosphorylation
PCR	Polymerase chain reaction
$PM_{2.5}$	Particulate matter (< 2.5 µm)
PM_{10}	Particulate matter (< 10 µm)
PPi	Inorganic phosphate
ROS	Reactive oxygen species
SOD	Superoxide dismutase
TCA	Tricarboxylic acid

Abstract

Introduction: Mitochondria are involved in many processes that are essential to cellular function. However, the relations between exposure to environmental stressors during early life and the mitochondrial phenotype remain poorly understood.

Objectives: During this master thesis research project, I aimed to characterize placental mitochondria on multiple biological levels and investigated whether changes in these characteristics are associated with tobacco smoke and air pollution (AP) exposure during pregnancy. Additionally, key methodological aspects and issues regarding the determination of mitochondrial characteristics were explored in depth.

Methods: From the ENVIR*ON*AGE birth cohort, 60 mother-newborn pairs were selected based on the mother's exposure levels to tobacco smoke and air pollutants ($PM_{2.5}$ and BC) during the pregnancy. Three groups were defined (n = 20 / group): mothers that smoked extensively during the pregnancy ("Smokers"), non-smokers with low AP exposure levels ("Controls") and non-smokers with high AP exposure levels ("Air Pollution"). Placental mitochondrial DNA (mtDNA) content was determined by RT-qPCR, with significant differences between groups ($p < 0.05$) being identified using Dunnett's test for multiple comparisons. DNA methylation levels of two mitochondrial genes (*D-loop*, *LDLR2*) and four nuclear genes (*DNA2*, *PINK1*, *POLG1*, *POLG1 exon 2*) were quantified by bisulphite pyrosequencing and subsequently analysed using linear mixed effect models.

Results: The "Smokers" group showed significantly lower placental mtDNA content compared with the "Control" group ($\beta = -57.5\%$, $p < 0.01$). A similar trend was observed for the "Air Pollution" group but was not statistically significant ($\beta = -7\%$, $p = 0.92$). Regarding gene-specific DNA methylation, a significant increase in methylation levels was observed in the *D-loop* region of the mtDNA in both the "Smokers" ($\beta = +0.40\%$, $p = 0.02$) and "Air Pollution" ($\beta = +0.61\%$, $p < 0.01$) group while a similar positive trend was found for the *LDLR2* region of the mtDNA ($\beta = +1.13\%$, $p = 0.20$ for "Air Pollution", $\beta = +0.17\%$, $p = 0.81$ for "Smokers"). For the nuclear genes, methylation on the *POLG1* promotor was significantly higher in the "Air Pollution" group ($\beta = +0.77\%$, $p < 0.01$), whereas *PINK1* methylation was higher in the "Smokers" group ($\beta = +0.76\%$, $p = 0.02$). Furthermore, non-linearized mtDNA showed incomplete bisulfite conversion and lead to overestimations of mtDNA methylation. Average methylation in the *LDLR2* region of the mtDNA was higher in non-linearized mtDNA than in linearized mtDNA (12.52% vs 3.99%, $p < 0.01$) whereas a less pronounced effect was observed for the *D-loop* region (4.97% vs 3.20%, $p < 0.01$).

Conclusions: Our findings show significant associations between environmental exposures during early life and placental mitochondrial characteristics, as both mtDNA content and mtDNA methylation were significantly different between the exposure groups. These associations suggest that exposure to stressors such as tobacco smoke and air pollution during pregnancy influences mitochondrial function in the placenta. Additionally, our data highlights several crucial methodological considerations that should be taken into account when assessing mtDNA content and mtDNA methylation.

Introduction

Mitochondria are intracellular organelles that are essential for cellular energy provision. They also play a critical role in calcium homeostasis, oxidant signaling, apoptosis, regulation of cell proliferation, and metabolism. Given that every cell of the body is dependent on energy metabolism, it is intuitive that mitochondria play an important role in disease processes.

Mitochondrial function

The primary function of mitochondria is the production of adenosine triphosphate (ATP), the single most important energy carrier molecule in the cell. ATP has a central role in different physiological processes such as metabolism, muscle contraction, and neurotransmission. Most crucially, the role of ATP as a substrate for phosphorylation reactions reveals its central role in a multitude of cellular signaling and regulation pathways. Mitochondrial function is often defined as the ability of the organelles to produce ATP, as it is the molecule that drives most cellular work. Thus, ATP generation is of critical importance to mitochondrial function.

The production of ATP requires disruption of the chemical bonds in adenosine diphosphate (ADP) and the addition of a third phosphate group. To complete this reaction, energy is required. In mammals, energy is predominantly produced by aerobic respiration (**Figure 1**), using glucose obtained from the diet as the primary source. Respiration is initiated in the cytosol, where two pyruvate molecules are produced from one glucose molecule during glycolysis. Additionally, two molecules of ATP are formed. Following glycolysis, pyruvate is transported into the mitochondrial matrix, where it is converted into Acetyl CoA by an oxidative reaction. In turn, Acetyl CoA forms an entry point for the tricarboxylic acid (TCA) cycle (also known as the citric acid or Krebs cycle). The first reaction of the TCA cycle converts Acetyl CoA into citrate and is catalyzed by citrate synthase, an enzyme that is often used in the characterization mitochondrial function. For every molecule of glucose, two ATP molecules are produced during the TCA cycle. However, most energy that is obtained during the TCA cycle is used to transfer electrons onto electron-carriers (FAD and NAD^+), thereby producing reduced power in the form of NADH and $FADH_2$ molecules. The reduced coenzymes are subsequently used during oxidative phosphorylation (OXPHOS), where the high-energy electrons they carry are shuttled into the electron transport chain (ETC) (1).

The process of OXPHOS is the most important cellular source of ATP, which means that mitochondrial function is often defined as the efficiency of this very process. It is easy to see why, since a maximum of 26 to 28 molecules of ATP can be produced during OXPHOS alone, thereby vastly outweighing the number of ATP molecules produced during glycolysis and the citric acid cycle combined. The process is powered by a series of mitochondrial enzyme complexes located in the inner mitochondrial membrane, which catalyze a set of reactions that result in the formation of a transmembranary proton gradient. The resulting protonmotive force is then coupled to an energy-producing mechanism based around chemiosmosis. The transport of protons from the intermembrane space into the mitochondrial

matrix is facilitated by ATP synthase (sometimes also called complex V of the ETC), and this proton flow along the gradient is used to phosphorylate ADP molecules, thereby assembling cellular energy in the form of ATP (1).

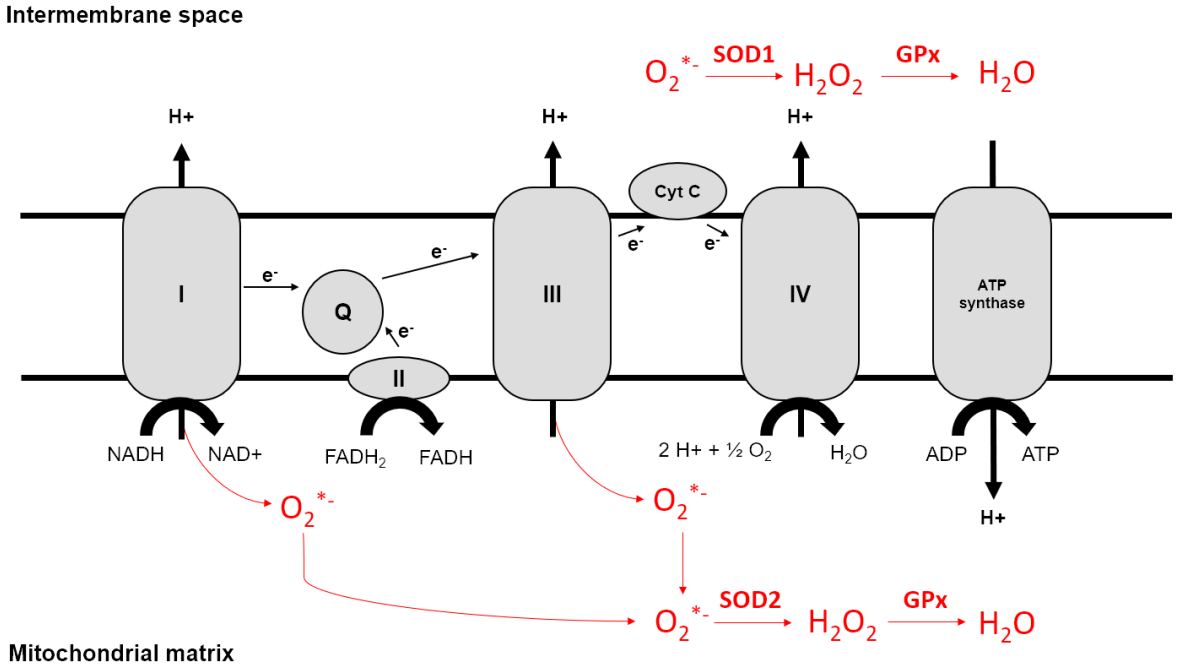

Figure 1: *Schematic overview of the reactions of the electron transport chain (ETC). Electron leakage from involved complexes leads to the formation of superoxide (O_2^{*-}) molecules. Reactive oxygen species (ROS) molecules can be scavenged by ROS mediating systems localized to the mitochondrial matrix and intermembrane space. Abbreviations: Q: Quinone, Cyt C: Cytochrome C, SOD: superoxide dismutase, GPx: glutathione peroxidase. Figure adapted from Li et al. (2013) (2).*

Although aerobic respiration is a remarkably efficient energy conversion process, the electron transport chain is not perfect. Electrons can leak from complex I and complex III and directly react with oxygen to form superoxide (O_2^{*-}) molecules, due to the nature of oxidation-reduction reactions (3). It is estimated that ~1-2 % of cellular oxygen forms O_2^{*-} molecules during cellular respiration (3). In addition to O_2^{*-} formation due to electron leakage from the ETC, superoxide dismutase (SOD) enzymes localized to the mitochondrial intermembrane space and mitochondrial matrix convert O_2^{*-} into H_2O_2, which can subsequently be converted into H_2O by enzymes such as glutathione peroxidases. Although H_2O_2 is less reactive than other reactive oxygen species (ROS) forms, excessive O_2^{*-} and H_2O_2 levels in proximity to mitochondrial iron- and sulphur-containing proteins leads to an environment where highly-reactive hydroxyl radicals (OH^*) can be formed through the Fenton reaction (4). High concentrations of ROS molecules can be detrimental to cellular function, since they can cause oxidative damage to essential biomolecules such as lipids, proteins and nucleic acids.

Despite their harmful properties, ROS should also be regarded as physiologically relevant metabolites because of their roles in various intracellular signaling pathways (5). Thus, to maintain cellular homeostasis, ROS production is balanced by several antioxidant systems, resulting in a steady-state of oxidative balance. Mitochondria are heavily involved in this oxidative balancing act not only because of

their role in ROS production, but also because of the mitochondrial localization of ROS scavenging systems. As previously mentioned, isoforms of SOD enzymes are localized to both the mitochondrial matrix (SOD1) and the intermembrane space (SOD2) and convert superoxide molecules into less reactive H_2O_2, which is subsequently converted into H_2O. In heart mitochondria, this process is at least partially carried out by catalase enzymes (6). However, the enzymes that are most critical in fulfilling this function are glutathione peroxidases (GPx), which use reduced glutathione molecules (GSH) to detoxify potentially harmful levels of H_2O_2. Subsequently, glutathione reductase (GR) recycles the oxidized glutathione (GSSG) to recuperate the reduced form of glutathione (7). Finally, it is worth noting that in addition to this oxidative signaling role, mitochondria are also involved in the regulation of signaling pathways by other mechanisms such as calcium $(Ca)^{2+}$-regulated second messenger signaling pathways (8). In addition to their role in Ca^{2+} signaling, mitochondria are also involved in pathways that regulate the cell cycle, like the p53 signaling pathway (7), further highlighting their crucial role in cellular signaling.

Mitochondrial dysfunction

Given the many functions mitochondria have in the maintenance of the cellular energy homeostasis as well as their role in crucial signaling pathways, it is not surprising that malfunctioning of the organelles can be harmful to proper physiological function at multiple biological levels, from the cellular to the systemic level. Diseases can originate from genetic deficiencies in genes regulating mitochondrial function and can affect many different parts of the body such as the nervous system, skeletal and heart muscles, kidneys, liver, eyes and ears. Many mitochondrial disorders are often multisystemic, although some are tissue specific, such as optic neuropathy, sensorineural deafness and type 2 diabetes mellitus (9). Organs that are bioenergetically and metabolically active – such as the heart, as well as the brain - naturally depend heavily on the cellular functions that mitochondria provide and are thus severely affected by mitochondrial dysfunction (10, 11). Another metabolically active organ that is particularly sensitive to mitochondrial dysfunction is the placenta, as during prenatal development, mitochondrial dysfunction from both the foetal and maternal sides have been associated with deficiencies in placental growth and development (12, 13).

Cells contain many mitochondria (200 to 2000), and each mitochondrion contains multiple copies (2 to 10) of its own mitochondrial DNA (mtDNA). Consequently, every cell contains many copies of the mitochondrial genome. In contrast with the nuclear DNA, mitochondrial DNA is circular in structure. The mitochondrial DNA encodes for several proteins that are critical to the proper function of the ETC. Mutations can occur both in the mitochondrial DNA (mtDNA) itself (14), but also in genes related to mitochondrial function that are located on the nuclear genome (9). In the mitochondrial DNA, the rate of mutation is five to ten times higher than on the nuclear DNA (15), and mutations that affect mitochondrial tRNA or genes that encode for proteins of the ETC heavily impact mitochondrial function (14).

Another finding that highlights the relevance of mitochondrial function to human health, is the adverse effects that certain anti-retroviral therapies have on mitochondrial function. More specifically, the use of anti-retroviral therapies has been linked to depletion of mtDNA (16) and may partially explain some of

the adverse side-effects, such as lactic acidosis and myopathy (17, 18), observed in HIV-patients that undergo these treatments. Such observations clearly stress not only the harmful consequences of mitochondrial dysfunction, but also strongly indicate that external factors can induce mitochondrial malfunction. Exposure to several environmental stressors, such as heavy metals, can induce higher levels of oxidative stress and thereby disturb the cellular oxidative balance (19). Given the role of mitochondria as a hub for cellular oxidative signaling and balancing, it is not surprising that such disturbances have been associated with changes in mitochondrial function (20).

Environmental stressors & health impact

One of the most important environmental pollutants that affects human health is ambient air pollution. Air pollution can be defined as the occurrence of particles in the atmosphere at concentrations high enough to be damaging to human health, to ecosystems or to human-made materials. Major air pollutants include carbon oxides, sulfur dioxide and sulfuric acids, ozone, volatile organic compounds, particulate matter and black carbon. Particulate matter is defined as solid particles that are small enough to be suspended in the atmosphere for long periods of time. Particles with a diameter smaller than 10 µm are defined as PM_{10}, while particles with a diameter smaller than 2.5 µm are defined as $PM_{2.5}$. These particles can consist of a wide variety of substances and originate both from natural (dust, sea salt, wild fires, etc.) and anthropogenic (burning of coal, motorized transport, etc.) sources (21). Black carbon (BC) makes part of $PM_{2.5}$, and specifically consists carbon structures. It originates from the incomplete combustion of organic fuels. Particulate matter has been shown to be able to penetrate into the lungs, where it can induce inflammation and endothelial dysfunction (22). Moreover, the smallest particles (ultrafine particles < 0.1 µm) can traverse the blood-lung barrier and enter the bloodstream causing a systemic inflammation.

The World Health Organization (WHO) estimates that 9 out of 10 people worldwide breathe air that is polluted beyond the recommended limit. On a global level, the organization estimates that air pollution causes more than 7 million deaths every year. In developed regions such as European countries, levels of ambient air pollution are on the decline. However, in many developing and Asian countries the levels of ambient air pollution are trending upwards. Furthermore, despite the lower overall levels of air pollution in Europe than in many developing regions, the European Court of Auditors (ECA) has estimated that air pollution causes about 400 000 deaths every year in the European Union (EU) alone. Given the massive scale of this global issue, research into the negative effects of air pollution on various aspects of human health is of high importance and necessary to raise awareness and improve public health.

Yet, despite this global relevance, investigations into the health effects of air pollution exposure during the most vulnerable stages in life, the *in-utero* period, are still relatively scarce. In recent years, prenatal exposure to ambient air pollution has been associated with increased risk of low birth weight at term (23, 24) and decreased newborn telomere length, a validated marker of biological ageing, in both cord blood and placenta (25). These observations coincide with the concept of the Developmental Origins of Health and Diseases (DOHaD), which states that biological changes during foetal life can result in

adaptations that form the origins of diseases later in life. As evidenced by decreased telomere length in foetal tissues (26), it is reasonable to suggest that prenatal exposure to ambient air pollution can influence the child's health later in life. Findings like these highlight the need to continue investigating the relationships between environmental factors and biological adaptations during early life, in order to better understand the concept of DOHaD.

Placental function is of critical importance during foetal development. The organ supplies the foetus with both nutrients and immune protection. Additionally, the placental barrier is an important defence mechanism against foetal exposure to a variety of harmful compounds (27). Cellular energy in the form of ATP is required to fuel these developmental processes, thereby stressing the key role of placental mitochondria during foetal development. Consequently, the use of mitochondrial characteristics as biomarkers of mitochondrial function is especially relevant when investigating the potential negative influences of prenatal exposures on health later in life.

Mitochondrial DNA content

One major mitochondrial characteristic is mitochondrial DNA content (mtDNA content), a relative measure of the quantity of the mitochondrial genome compared to the nuclear genome. The integrity of mtDNA is highly relevant to mitochondrial function, since complex I, III, IV as well as ATP synthase of the ETC all contain proteins synthesized from mtDNA sequences (28). The proximity of the mitochondrial genetic material to the O_2^{*-} and H_2O_2 molecules formed during cellular respiration makes the mtDNA especially vulnerable to oxidative damage. This vulnerability is further aggravated by the lack of protective features that the mitochondrial genome has as compared with the nuclear genome. In the nucleus, large amounts of genetic material are organized in the form of chromatin. By contrast, the mtDNA is relatively small and circular in form, and is not packaged in the same compact way. The mtDNA is therefore structurally more open and more likely to be damaged by reactive molecules. Repair of the mtDNA is also not coordinated in the same way as it is for the nuclear genome. Although mtDNA is repaired by the base excision repair (BER) pathway, other forms of mtDNA repair are limited (29). All of these properties are unique to the mtDNA, and combined they result in the fact that the mitochondrial genome is damaged more easily and remains damaged for a longer period as compared with the nuclear genome (30). In the context of epidemiological research, both this vulnerability and persistence of mtDNA damage makes mtDNA content an especially appealing characteristic to investigate.

Nuclear and mitochondrial DNA methylation

Another molecular mechanism that impacts mitochondrial function are epigenetic alterations in the form of DNA methylation. Methylation of cytosine residues on DNA is one of the primary epigenetic mechanisms that influences the regulation of gene expression, with increased methylation levels (usually) being associated with repressed gene expression. Multiple studies have shown an association between prenatal exposure to air pollution and epigenetic alterations on nuclear genes in the placenta, both genome wide (31) as well as on specific DNA regions. More specifically, a link between

hypomethylation on the *LINE-1* retrotransposon and *in utero* exposure to particulate matter (32) suggests that particulate matter can induce developmental toxicity. Furthermore, the correlation between increased *APEX1 and OGG1* methylation and environmental exposure (33) indicates that DNA repair mechanisms can be impaired. This conclusion is further strengthened by an observation from the ENVIR*ON*AGE birth cohort that reveals an association between alterations in methylation on *APEX1* and *OGG1*, which are also key genes involved in DNA repair pathways and ambient air pollution (34). To summarize, DNA methylation is relevant to the regulation of gene expression and foetal development and is impacted in different ways by exposure to environmental stressors.

While the relevance of DNA methylation in the regulation of genes on the nuclear genome is well established, controversy exists regarding methylation on the mitochondrial DNA (**Table 1**). Over the years, many different methods have been used to quantify mtDNA methylation. The earliest studies that investigated mtDNA methylation used methyl-specific restriction enzyme-based methods and reported very low levels of methylation (2 – 5 %) (35, 36). Later studies made use of more sensitive techniques such as methylated DNA immunoprecipitation (37, 38), mass spectrometry (39) or ELISA (40) to investigate mtDNA methylation, and reported higher methylation values (up to 13 – 25%). Furthermore, studies that use bisulfite sequencing – currently regarded as the gold standard method to quantify DNA damage - have reported relatively higher levels of methylation (up to 10 – 37%) (41-43). Based on the observations made using the more modern methodologies, one would conclude that methylation on the mitochondrial genome is relevant to the regulation of mitochondrial function. However, a set of recent studies have revealed crucial methodological flaws in previous bisulphite sequencing experiments (44, 45). Recent findings suggest that bisulfite conversion efficiency is negatively affected by the secondary structure of the mitochondrial DNA, leading to incomplete bisulfite conversion and therefore overestimations of mtDNA methylation levels. When linearizing the mitochondrial DNA before bisulfite conversion, observed methylation on the mitochondrial genome was drastically lower, to the point of approaching the limit of detection. As a result, both the overall existence and relevance of mitochondrial DNA methylation is currently a topic of debate. Nonetheless, it should be noted that Liu *et al.* observed that levels of mtDNA methylation in human saliva samples were not impacted by overestimation due to poor bisulfite conversion (44), indicating that the degree to which mtDNA methylation was previously overestimated may be both region and tissue-specific, a conclusion further supported by findings from van der Wijst *et al.* (46).

Table 1: Overview of previous investigations into DNA methylation on the mitochondrial genome.

Tissue	Methodology	Observation	Target region	Reference
Human fibroblasts	Methyl sensitive restriction enzymes	2 - 5% methylation.	CCGG sites on the mitochondrial genome	Shmookler Reis *et al.*, 1983 (35)
Mouse cells	Methyl sensitive restriction enzymes	2 – 5 % methylation.	CCGG sites on the mitochondrial genome	Pollack *et al.*, 1984 (36)
Mouse and human cell lines (HCT116)	MeDIP + RT-qPCR	10- to 20-fold enrichment of anti-5mC immunoprecipitated mtDNA	Whole mitochondrial genome	Shock *et al*., 2011 (37)
Piglet muscle	MeDIP + RT-qPCR	~ 0.05 to 0.40 % enrichment relative to input	mtDNA control region	Jia *et al*., 2013 (38)
Mouse neural cells	ELISA	~ 0.05 – 0.30 units	Whole mitochondrial genome	Dzitoyeva *et al*., 2012 (40)
Human lymphoblastoid cell line	Mass spectrometry	~ 13 – 25 % methylation	Whole mitochondrial genome	Infantino *et al*., 2011 (39)
Human placenta	Bisulfite sequencing (mtDNA not linearized)	~ 5 – 14 % methylation (MT-RNR1) ~2 – 5 % methylation (D-loop)	MT-RNR1, D-loop	Janssen *et al.*, 2015 (42)
Human muscle	Bisulfite sequencing (mtDNA linearized)	~ 0 – 1 % methylation	D-loop, MT-RNR1 (12S), 16S, ND5, Cyt b	Mechta *et al.*, 2017 (45)
Human blood (buffy coat)	Bisulfite sequencing (mtDNA not linearized)	~ 2 – 7% methylation	MT-TF, D-loop, MT-RNR1	Byun *et al.*, 2013 (41)
Human whole blood and saliva	Bisulfite sequencing (mtDNA linearized)	~ 0 – 2 % methylation	D-loop, MT-RNR1, MT-RNR2, ND1, COX1, ND1, ND3, ND4, ND5, CYTB	Liu *et al*., 2016 (44)
Human cell lines (HCT116, HeLa, SKOV3, C33A, mtDNA disease fibroblast)	Bisulfite sequencing (mtDNA linearized)	~ 0 – 20 % methylation	D-loop, COX2	van der Wijst *et al.*, 2017 (46)
Human cell lines (HCT116)	Bisulfite sequencing (mtDNA linearized)	~ 0 – 0.66 % methylation	Whole mitochondrial genome	Hong *et al.*, 2013 (47)
Human skin fibroblasts, Human cell lines (HeLa, osteosarcoma) and mouse cell lines (3T3-L1)	Bisulfite sequencing (mtDNA not linearized)	~ 10 – 37 % methylation	D-loop	Belizzi *et al.*, 2013 (43)
Human iPS cells and mouse liver	Bisulfite sequencing (mtDNA linearized)	~ 0 – 0.65 % methylation	Whole mitochondrial genome	Owa et al., 2018 (48)

Aims and objectives

During this master thesis research project, the aim was to characterize placental mitochondrial function, and investigate correlations between the determined characteristics and *in utero* exposure to environmental stressors. The exposures of interest were particulate matter with a diameter smaller than 2.5 µm ($PM_{2.5}$) and black carbon (BC), both are common forms of ambient air pollution. The influence of maternal smoking habits during pregnancy were also investigated, since smoking can be regarded as a personalised form of high-dosage air pollution. According to the US Department of Health and Human Service, tobacco smoke contains over 7000 compounds, 70 of which have carcinogenic effects. Besides mtDNA content, we also aimed to assess how environmental exposures affect methylation levels on both nuclear and mitochondrial DNA regions that are relevant to mitochondrial function. The DNA regions that were selected for quantification are relevant to the maintenance and replication of the mtDNA, or to the regulation of mitochondrial integrity in general.

Two of the target regions were located on the displacement loop (D-loop) region of the mitochondrial genome, with one region located on the heavy chain (hereafter referred to as "*D-loop*") and one was located on the light chain (hereafter referred to as "*LDLR2*"). The D-loop region does not code for any gene products. Nonetheless, it is the region on the mitochondrial genome where mtDNA replication is initiated. The final mtDNA region that was investigated was located on a gene that codes for the mitochondrially encoded ribosomal 12S RNA ("*MT-RNR1*"), which is an essential part of the small subunit of the mitochondrial ribosomes that translate mtDNA-encoded RNA into proteins. On the nuclear genome, the *POLG1*, *PINK1* and *DNA2* genes were selected as genes of interest. *POLG1* encodes for the catalytic subunit of the only mitochondrial DNA polymerase: DNA polymerase-γ. In addition to its role in the replication of mtDNA, DNA polymerase -γ is also involved in the maintenance of mtDNA integrity by participating in the base excision repair pathway (49). The *DNA2* gene is also related to the replication of mtDNA, as it encodes for a helicase involved in mtDNA replication machinery. Finally, although the *PINK1* gene is not involved in mtDNA replication, its gene product (PTEN induced kinase 1) is involved in protecting mitochondria from malfunctioning during periods of excessive cellular stress (50). Additionally, we aimed to investigate how secondary mtDNA structure influenced bisulfite conversion efficiency (and by extension on the observed methylation levels) on the placental mitochondrial genome.

To achieve all these different aims within the scope of this master thesis research project, a case-control study was performed. We used a subset of the ENVIR*ON*AGE birth cohort to create three different exposure groups divided based on the maternal exposure to both air pollution and tobacco smoke during the pregnancy (i.e. a control group, a smokers group, and an air pollution group; n = 20 / group). Based on previous observations within the ENVIR*ON*AGE birth cohort (51, 52) - in addition to those from other cohorts (53) - *in utero* exposure to tobacco smoke and increasing levels of air pollution was expected to be associated with a decline in placental mtDNA content. Taking these findings into account, we hypothesized that *in utero* exposure to both particulate matter and tobacco smoke would be associated with increased levels of DNA methylation on the previously described DNA regions.

Materials & Methods

Study population

This study made use of samples from the ongoing ENVIR*ON*AGE (ENVIRonmental influence *ON* early AGEing) birth cohort study. Recruitment of participants for the birth cohort started in February 2010 and has continued to this date. Mother-newborn pairs were recruited when they arrived for delivery at the Hospital East-Limburg (ZOL) in Genk (Belgium). Mothers who did not have planned caesarean sections and who were able to fill out the Dutch language questionnaires were eligible to participate in the study. Participating mothers provided written informed consent upon arrival in the hospital. Several questionnaires were filled out in the postnatal ward after delivery. The questionnaires were set up to gather detailed information regarding maternal age, health status, pre-pregnancy body mass index (BMI), maternal education, socio-demographic status, occupation, self-reported smoking status, alcohol consumption, place of residence, medication use, parity, newborn's ethnicity and other lifestyle factors. Maternal education status was categorized as "Low" (no diploma or primary school), "Middle" (high school) or "High" (college or university degree). Based on the native country of the newborn's grandparents, their ethnicity was classified. Newborns were considered European-Caucasian when two or more grandparents were of European origin, and non-European when at least three grandparents were of non-European origin. Information about tobacco smoke exposure was self-reported by the mothers. Mothers were asked whether they continued smoking during pregnancy, whether they smoked before pregnancy and whether they stopped when pregnant, or whether they never smoked in their life. Mothers that reported smoking at any point in their life, filled out the number of smoking years and the number of cigarettes smoked per day before and during pregnancy. All medical records during and after pregnancy were accessible, including foetal ultrasound data, and the anthropometric data was used to double-check the data obtained from the questionnaires. Up to now, more than 1800 mother-newborn pairs have been recruited for the cohort. The total study population is representative for all births in Flanders regarding maternal age, education and parity as well as new-born's sex, ethnicity and birth weight (25).

A selection of 60 mothers-newborn pairs was made based on their level of exposure to tobacco smoke and air pollution (AP) during the pregnancy. 20 mothers with the highest reported packyears (packs per day multiplied by the number of years they report smoking) and with an average number of cigarettes smoked per day during the pregnancy above the third quartile (10 cigarettes per day) were selected (hereafter referred to as "Smokers" group). The "Smokers" group was matched on age and newborn's sex with a group of 20 non-smoking mothers with the lowest exposure to $PM_{2.5}$ and black carbon (BC) during the third trimester as well as during the entire pregnancy (hereafter referred to as "Control" group). Finally, the "Control" group was matched on age and gender with a group of 20 non-smoking mothers that were exposed to the highest $PM_{2.5}$ and BC levels during the third trimester as well as during the entire pregnancy (hereafter referred to as "Air Pollution" group).

Exposure assessment

A spatiotemporal interpolation method (Kriging) (54) was used to calculate daily exposure levels (µg/m^3) to $PM_{2.5}$ and black carbon (BC) during the prenatal period. Exposures were estimated for the entire pregnancy as well as for the third trimester (27 weeks after conception until delivery) specifically, with the date of conception being determined based on ultrasound data. Home addresses were geocoded for each study participant. The interpolation method considers land-cover data obtained from satellite images (CORINE land-cover data set) and pollution data from fixed monitoring stations (n = 34) in combination with a dispersion model (55). For Flanders, the validation statistics of the interpolation tool gave a spatiotemporal explained variance of more than 0.80 for $PM_{2.5}$ and 0.74 for BC. Daily concentrations of air pollutants at the mother's home address during pregnancy (prenatal exposure) were calculated. Complete information for the residential address during pregnancy was obtained by questionnaire and checked with hospital records. For those who moved residence during pregnancy, we calculated daily exposures allowing for the changes in address during this period.

Sample collection & preparation

Within 10 minutes after delivery, a placental biopsy of approximately 1-2 cm^3 in size was taken from the foetal side of the placenta. The largest umbilical cord artery was used as the reference point from which the entry point was defined. The biopsy was taken to the right of entry point, 4 cm away from the umbilical cord and 1 cm below the chorioamniotic membrane. The biopsy was deep-frozen within 10 minutes of delivery and stored at -80°C until further use for DNA extraction.

A small amount of biopt tissue (10 mg) was washed with phosphate-buffered saline (PBS, 137 mmol/L NaCl, 2.7 mmol/L KCl, 10 mmol/L Na_2HPO_4 and 1.8 mmol/L KH_2PO_4) to remove excess blood. The tissue was shredded using a Mixer Mill MM400 (Retsch Benelux Verder N.V., Aartselaar, Belgium) using stainless-steel beads. DNA was extracted from the homogenized tissue using the QIAamp DNA Mini Kit (Qiagen Inc., Venlo, the Netherlands), according to the manufacturer's instructions. Concentrations of extracted DNA were determined based on the spectral absorbance of the eluate at 260 nm (NanoDrop ND 1000, Thermo Fisher Scientific, Geel, Belgium). Purity of the extract was assessed based on the 260/230 nm and 260/280 nm absorbance ratios. Finally, extracted DNA samples were stored at -80°C until further use.

mtDNA content analysis

Placental mtDNA content was defined as the ratio between one single-copy mitochondrial gene copy number to one single-copy nuclear control gene and measured using a real-time quantitative polymerase chain reaction (RT-qPCR) assay. Two sets of genes were tested (all PCR primers used are listed in **Supplemental Table 1**). The first set of genes used to quantify mtDNA content was *ND-1* for the mitochondrial gene and *RPLP0* as the nuclear reference gene, a combination previously used within the research group (51). When using comparative genomics techniques (BLAST) to compare the *ND-1*

amplicon (115 bp) against the latest human reference genome assembly (GrCh38.p12), it was revealed that the amplicon sequence shows similarity with a DNA segment on the nuclear genome. Nonetheless, the similarity starts from the 7th base pair only, meaning that the first 6 base pairs of the forward primer sequence do not match. This information indicates that despite the sequence similarity, there should be no nonspecific amplification since the forward primer is unlikely to bind to the homologous sequence on the nuclear genome. Nonetheless, a second primer set that made use of a DNA segment very specific to the mitochondrial genome (hereafter referred to as "*hmito3*"), as described by Malik et al. (56), was also tested for comparison. For this assay, a segment of the *HBB* gene was used as the nuclear reference segment.

Samples were diluted to 2.5 ng/µL in two steps to ensure accurate final concentrations using a Quant-iT dsDNA broad range Assay Kit (Thermo Fisher Scientific, Geel, Belgium), according to the manufacturer's instructions. The PCR reaction mixture consisted of 2.5 µL of DNA (2.5 ng/µL), 5 µL of Fast SYBR Green I dye (2x), 300 nM of forward and reverse primers (0.3 µl each) and 1.9 µL of RNase-free water. To reduce between-run variability, the two genes were measured on the same plate, in triplicate 384-well format. Real-time PCR was performed using the 7900HT Fast Real-Time PCR System (Applied Biosystems, Foster City, USA) with following thermal cycling profile: 20 s at 95°C (activation), followed by 40 cycles of 1 s at 95°C (denaturation), and 20 s at 60°C (annealing/extension), ending with melting curve analysis (15 s at 95°C, 15 s at 60°C, 15 s at 95°C). The process the results, qBase software (Biogazelle, Zwijnaarde, Belgium) was used, which automatically averages triplicate measurements that pass quality control and normalizes the data to the nuclear reference genes. The PCR products were visually checked for the correct amplicon size by agarose gel electrophoresis.

DNA methylation analysis

To linearize circular mitochondrial DNA, BamHI restriction enzymes were used. BamHI is an endonuclease that recognizes and cuts DNA strands at a specific 6 bp-long recognition site: GGATCC. Since this recognition sequence is palindromic, the enzyme is able to cut both DNA strands at the same time, resulting in a double-stranded DNA break. The sequence occurs only once in the mitochondrial genome (starting at the 14 257th base pair), meaning that treatment of the circular mitochondrial DNA with the restriction enzyme results in one linear double-stranded mitochondrial DNA molecule. The digestion was performed using 600 ng of extracted DNA. Samples were incubated with the FastDigest BamHI enzyme (Thermo Fisher Scientific, Geel, Belgium) in a universal FastDigest buffer for 10 minutes at 37°C, according to the manufacturer's instructions. The digesting reaction was then inactivated by incubating the reaction mixture for 5 minutes at 80°C. Finally, 600 ng of BamHI-digested DNA was used with the EZ-96 DNA methylation Gold kit (Zymo Research, Orange, USA) to perform the bisulphite conversion according to the manufacturer's instructions. To limit the number of freeze-thaw cycles, the bisulfite converted DNA samples were split into separate 96-well work plates (one plate per planned methylation assay). Each work plate contained 1 µL of every DNA sample diluted in 8 µL of RNase-free water (as part of the PCR master mix). Work plates were stored at -80°C until further use.

Methylation on CpG sites in various regions on both nuclear (*POLG1*, *PINK1*, *DNA2*) and mitochondrial (*D-loop*, *LDLR2*, *MT-RNR1*) DNA were investigated. Detailed information regarding primer sequences can be found in **Supplemental Table 2**. Prior to pyrosequencing, the regions of interest were PCR amplified using PyroMark PCR kits (Qiagen Inc., Venlo, The Netherlands) in a thermal cycling device (C1000 Thermal Cycler, Bio-Rad Laboratories, Temse, Belgium). The 25 µL reaction mixture contained 1 µL of bisulphite treated DNA, 12.5 µL of the PyroMark PCR Master Mix (2x), 2.5 µL CoralLoad Concentrate (10x), 0.5 µL each of the forward and reverse primer (10 µM), and 8 µL of RNase-free water. The thermal cycling conditions were as follows: 15 min at 95°C (activation), followed by 45 cycles of 30s at 94°C (denaturation), 30 s at 58.7°C-53°C (annealing temperatures were assay-dependent, see **Supplemental Table 2**) and 30 s at 72°C (extension), ending with a final round of extension (10 min at 72°C). PCR products were visualized using gel-electrophoresis on a 2% agarose gel stained with GelRed Nucleic Acid Gel Stain (Biotium, Brussels, Belgium). Amplified PCR products were sequenced by pyrosequencing using a PyroMark Q48 Autoprep system (Qiagen, Inc., Venlo, The Netherlands), using a sequence primer concentration of 4 µM. The degree of methylation was defined as the percentage of methylated cytosines over the sum of methylated and unmethylated cytosines. The samples were measured over two separate 48-well sequencing discs. Efficiency of the bisulfite conversion process was assessed using non-CpG cytosine residues within the sequence to analyze. We used 0% (PSQ-T oligo: 5′-TTGCGATACAACGGGAACAAACGTTGAATTC-3′) and 100% (PSQ-C oligo: 5′-TTGCGATACGACGGGAACAAACGTTGAATTC-3′) DNA methylation control oligos as template (10 µM). The sequence of the control oligo was the following: 5′-AACGTTTGTTCCCGT-3′. Pyrosequencing of the control oligos was performed with the following sequence to analyze: C/TGTAT. Using universal DNA samples present on every pyrosequencing disc, inter-run differences were assessed. Final methylation values were adjusted for this variation using inter-run variation correction factors calculated from the obtained methylation values for the universal DNA samples.

Optimization of pyrosequencing assays

Bisulfite pyrosequencing is a sensitive and accurate method to determine DNA methylation levels. After bisulfite conversion of the template DNA, all non-methylated cytosine residues in the template DNA are converted into uracil residues. After PCR, this results in new bisulfite-treated template strands on which all non-methylated cytosine residues are replaced with thymine residues, whereas the methylated cytosine residues are not replaced. Following bisulfite treatment and PCR, the template amplicon is sequenced by pyrosequencing, as schematically represented in **Figure 2**. The percentage methylated cytosine on the variable position is calculated based on the signal ratio between thymine and cytosine residues on the variable positions.

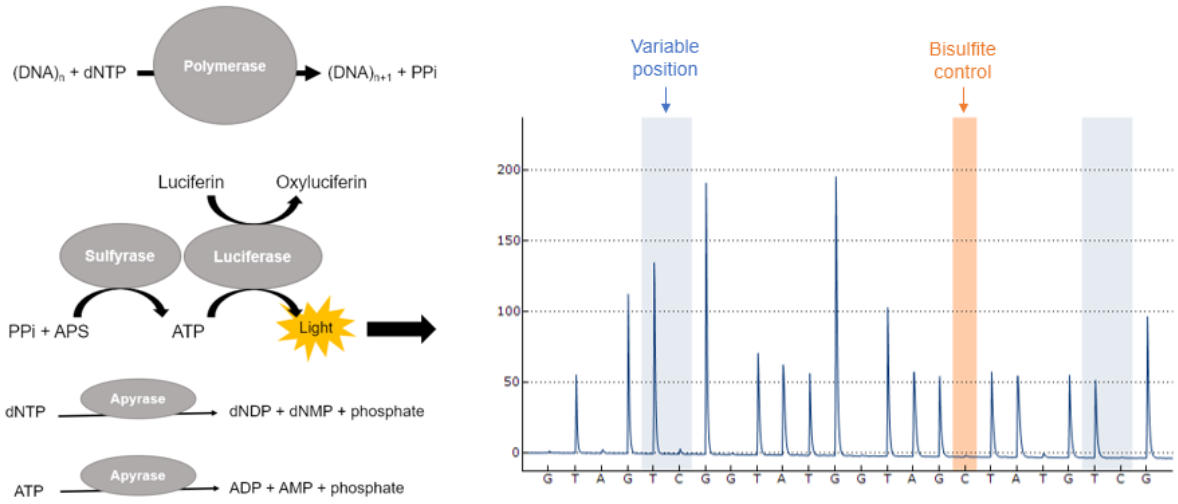

Figure 2: Schematic overview of the pyrosequencing methodology, as it is implemented in the Q48 Autoprep pyrosequencing system by Qiagen Inc. (Venlo, The Netherlands). *As a specific nucleotide is added by a polymerase, pyrophosphate (PPi) is released. By a combination of the activities of sulfyrase and luciferase enzymes, this PPi release is observed as a light signal, with the intensity of the signal being proportional to the amount of the nucleotide being added to the sequence. Leftover reaction products and reagents are removed by apyrase enzymes.*

Assay optimization is of critical importance to avoid bisulfite pyrosequencing pitfalls. Sequencing assay primer sets must be thoroughly designed, optimized and tested to prevent non-specific PCR amplification and pyrosequencing background signal. Additionally, the final assay has to provide sufficient peak-height during the sequencing process, since low signal-to-noise ratios will result in inaccurate quantification on variable positions. The last factor that must be taken into consideration is bisulfite conversion efficiency. Inefficient bisulfite conversion of the template DNA leads to the presence of non-methylated cytosine residues that otherwise would have been converted into uracil residues. Poor bisulfite conversion therefore leads to an overestimation of methylation values. Consequently, it is crucial that bisulfite conversion efficiency is optimal.

To account for these pitfalls, multiple controls were included during the optimization phase of this research project. Specificity of the assays was checked using comparative genomics techniques (BLAST) to screen the PCR amplicons for sequence similarity with DNA segments outside the region of interest. Comparisons were made against the most recent version of the human reference genome assembly (GrCh38.p12). The efficiency of the bisulfite conversion process was determined by assessing the cytosine to thymine signal ratio on bisulfite control positions in the sequence to analyze. Background signal was assessed by four different negative controls: the PCR template only, the sequencing primer only, a negative PCR, and finally the combination of a negative PCR and the sequencing primer. Depending on which negative controls or combination of controls a signal was observed, the cause of the background signal can be narrowed down (**Table 2**). Once the source of the background signal is determined, further optimization steps can be taken to resolve the issue, depending on the nature of the

problem. For the assays that were used during this study, there was no need for optimizations specifically aimed at reducing background signal.

Table 2: Overview of bisulfite sequencing controls and possible actions to take, should background signal be observed.

Control	Cause of background	Possible solution
Template only	Template strand forms secondary structures, allowing extension from the 3' end.	▪ Redesign PCR primers ▪ Sequence the complementary strand
Sequence primer only	Sequence primer dimers can be formed, resulting in 5' overhangs with 3' terminal match, which serve as a template for extension	▪ Redesign PCR primers ▪ Reduce sequencing primer concentrations
Negative PCR	PCR primer dimers can be formed, resulting in 5' overhangs with 3' terminal match, which serve as template for extension.	▪ Optimize PCR conditions to fully consume PCR primers ▪ Redesign PCR primers
Negative PCR + sequence primer	Sequence primer binds the biotinylated primers, resulting in stable 5' overhang with 3' terminal match, which serve as template for extension.	▪ Optimize PCR conditions to fully consume PCR primers ▪ Redesign PCR primers

Optimizing pyrosequencing assays to provide higher peak height can be less straightforward. During this study, initial runs of the *MT-RNR1* assay produced inadequate peak height. After testing the assay under numerous different conditions (general PCR optimization steps, using HPLC-purified primers, and increased sequencing primer concentration to 10 µM), it was concluded that the issue likely stemmed from the length of the PCR amplicon (431 bp). This proved problematic, since reducing the length of the amplicon inevitably resulted in reducing the specificity of the assay. As a solution to this problem, a nested PCR was performed, resulting in a shorter amplicon while maintaining specificity. Under these new conditions, the runs from the *MT-RNR1* assay did produce sufficient peak height to quantify methylation on the different CpG sites.

Statistical analysis

All statistical analyses were performed using R version 3.5.3 (R Core Team, Vienna, Austria). Residuals for all analyses were visually inspected for deviations from homoscedasticity or normality. Comparison of characteristics between the exposure groups with the control group were tested using a Chi-squared test for categorical variables and a Student's t-test for numerical variables. Pearson correlation coefficients were used to determine the relationship between the two tested mtDNA content assays and a Bland-Altman plot was used to compare the two methods. To determine significant differences in mtDNA content between the exposure groups (at a 95% confidence level), one-way ANOVA was used. Afterwards, Dunnett's test for comparisons was used to make pairwise-comparisons between the means of the "Air Pollution" and "Smokers" groups compared with the means of the "Control" groups. To compare methylation levels between linearized and non-linearized mtDNA, a Student's t-test was used. With linear mixed effect analysis, we took into account each CpG position and tested the associations between gene-specific DNA methylation and exposure group. All linear mixed models were constructed

using the *lme4* package (57), with two main models being constructed for every target region: one for the comparison between the “Control” and “Smokers” group and one for the comparison between the “Control” and “Air Pollution” group. To obtain p-values, the *lmerTest* package was used (58). Main models included exposure group, CpG site, date of delivery, maternal education status, maternal parity status, maternal pre-gestational BMI, the newborn’s ethnicity and the newborn’s gestational age as fixed effects. As for random effects, a random intercept was included for individuals. The interaction between exposure group and CpG site was tested, but only included in the main models when the interaction term was significant ($p < 0.05$). In those cases, a post-hoc analysis (Dunnett’s test for multiple comparisons between the exposure groups and the “Control” group) was performed to determine significant differences in methylation on specific CpG sites between the exposure groups at a 95% confidence level. A sensitivity analysis was performed by using the raw methylation values (unadjusted for inter-run variation) with the pyrosequencing disc identifier as a random effect in the models to account for inter-run differences.

Results

Study population characteristics

The characteristics of the study population are summarized in **Table 3**. Data is categorized by exposure group: non-smokers with low levels of air pollution exposure (hereafter referred to as “Control”), non-smokers with high levels of air pollution exposure (hereafter referred to as “Air Pollution”) and those who have smoked during pregnancy (hereafter referred to as “Smokers”). The groups were matched for maternal age and the newborn’s sex so there were no differences in age or sex between groups. On average, mothers from all groups were 31 to 32 years old (ranging from 23 to 40 years old). Each group included 13 male and 7 female newborns. Average maternal pre-gestational BMI was comparable between the “Control” and “Smoker” groups (23.9 kg/m^2 and 24.0 kg/m^2 respectively), while being one unit lower in the air pollution group (24.0 kg/m^2). There was a significant difference in socio-economic status (proxied by maternal education status) between the groups. On average, mothers from the “Smokers” group had a lower educational status compared with mothers from the “Control” group. As expected, birth weight was lower in the “Smokers” group (3149 g) compared with the “Control’ group (although the difference was only borderline significant at a 95% confidence level ($p = 0.08$). For the “Air Pollution” group, average newborn birth weight was comparable to the “Control” group (3390 g). All groups were highly comparable regarding the average newborn’s gestational age (ranging between 35 and 41 weeks). For ethnicity, there were slight differences between the groups, with both the “Control” (25%) and “Air Pollution” (15%) groups counting more non-European newborns than the “Smokers” group (5%) although this difference was not significant ($p = 0.18$).

Average exposure to ambient air pollution during the entire pregnancy was significantly higher for the “Air Pollution” than for the “Control” group (16.0 µg/m^3 versus 10.6 µg/m^3 for $PM_{2.5}$, and 1.8 µg/m^3 versus 0.9 µg/m^3 for black carbon). Notably, air pollution exposure was also significantly higher for the “Smokers” group as compared with the “Control” group, but to a lesser extent than for the “Air Pollution” group (13.3 µg/m^3 versus 10.6 µg/m^3 for $PM_{2.5}$, and 1.3 µg/m^3 versus 0.9 µg/m^3 for black carbon). Similar trends regarding exposure levels were observed during the third trimester (**Table 3**). In the “Smokers” group, mothers had an average of 15 packyears and smoked 13.2 cigarettes per day on average.

Table 3: Maternal, newborn and exposure-related characteristics of the selected mother-newborn pairs, categorized by exposure group*. Asterisks (*) indicate significantly differences in characteristics between the exposure groups ("Air Pollution" and "Smokers") versus the "Control" group at a 95% confidence level using a Chi-squared test for categorical variables and a Student's t-test for numerical variables. Abbreviations: PM: Particulate Matter. BC: Black Carbon.*

Characteristics	**Number (%) or mean (±SD; range)**			
	Control (n = 20)	*Air Pollution (n = 20)*	*Smokers (n = 20)*	
Maternal				
▪ Age (years)	31 (24 - 40)	32 (24 - 40)	31 (23 - 40)	
▪ Pre-gestational BMI (kg/m^2)	23.9 (± 5.3)	22.9 (± 4.3)	24.0 (± 4.0)	
▪ Education				
- Low	1 (5%)	4 (20%)	12 (60%)	*
- Middle	8 (40%)	4 (20%)	7 (35%)	
- High	11 (55%)	12 (60%)	1 (5%)	
▪ Parity				
- 1	9 (45%)	6 (30%)	7 (35%)	
- 2	7 (35%)	12 (60%)	7 (35%)	
- ≥ 3	4 (20%)	2 (10%)	6 (30%)	
▪ Caesarean section	1 (5%)	1 (5%)	0 (0%)	
Newborn				
▪ Gender				
- Male	13 (65%)	13 (65%)	13 (65%)	
- Female	7 (35%)	7 (35%)	7 (35%)	
▪ Ethnicity				
- European	15 (75%)	17 (85%)	19 (95%)	
- Non-European	5 (25%)	3 (15%)	1 (5%)	
▪ Gestational age (weeks)	39.2 (37 - 41)	39.0 (35 - 41)	39.3 (36 - 41)	
▪ Apgar score (after 5 minutes)				
- ≥ 8	2 (40%)	1 (5%)	2 (10%)	
- 9	10 (10%)	5 (25%)	6 (30%)	
- 10	14 (50%)	14 (70%)	12 (60%)	
▪ Birth weight (g)	3394 (± 522)	3390 (± 401)	3149 (± 300)	
Exposure				
▪ $PM_{2.5}$ Exposure (µg/m^3)				
- Third trimester	7.3 (± 1.0)	22.5 (± 3.0) (*)	11.7 (± 4.4) (*)	
- Whole pregnancy	10.6 (± 1.7)	16.0 (± 1.4) (*)	13.3 (± 2.5) (*)	
▪ BC Exposure (µg/m^3)				
- Third trimester	0.7 (± 0.2)	1.9 (± 0.3) (*)	1.2 (± 0.4) (*)	
- Whole pregnancy	0.9 (± 0.1)	1.8 (± 0.3) (*)	1.3 (± 0.4) (*)	
▪ Smoking behaviour				
- Number of pack years	/	/	15.1 (± 3.5)	
- Number of cigarettes (/day)	/	/	13.2 (± 4.9)	

BamHI-based linearization of the circular mtDNA before bisulfite treatment had a significant impact on observed methylation values in two out of the three target regions (**Figure 2**). Across the two *LDLR2* CpGs that were investigated, mean methylation levels were relatively 66.3% lower in linearized than in circular mtDNA ($p < 0.001$). Similar effects were observed on the individual CpG sites. Notably, we observed relatively high levels of methylation on the first CpG on the *LDLR2* target region (9.38 %) compared with the second CpG (1.15%) on linearized mtDNA. In the *D-loop* region, mean methylation levels on each CpG were lower on linearized mtDNA, but reached significance on only one of the three individual CpG sites (CpG 3). However, average methylation across the CpGs was relatively 30% lower on linearized mtDNA compared with the untreated group ($p = 0.044$). Although significantly lower methylation levels were observed in the BamHI-treated group for the *LDLR2* and *D-loop* regions, similar effects were not observed for the *MT-RNR1* region: no significant differences regarding mtDNA methylation were observed on any of the three *MT-RNR1* CpG sites that were investigated, which might be due to the fact that methylation values were close to the limit of detection.

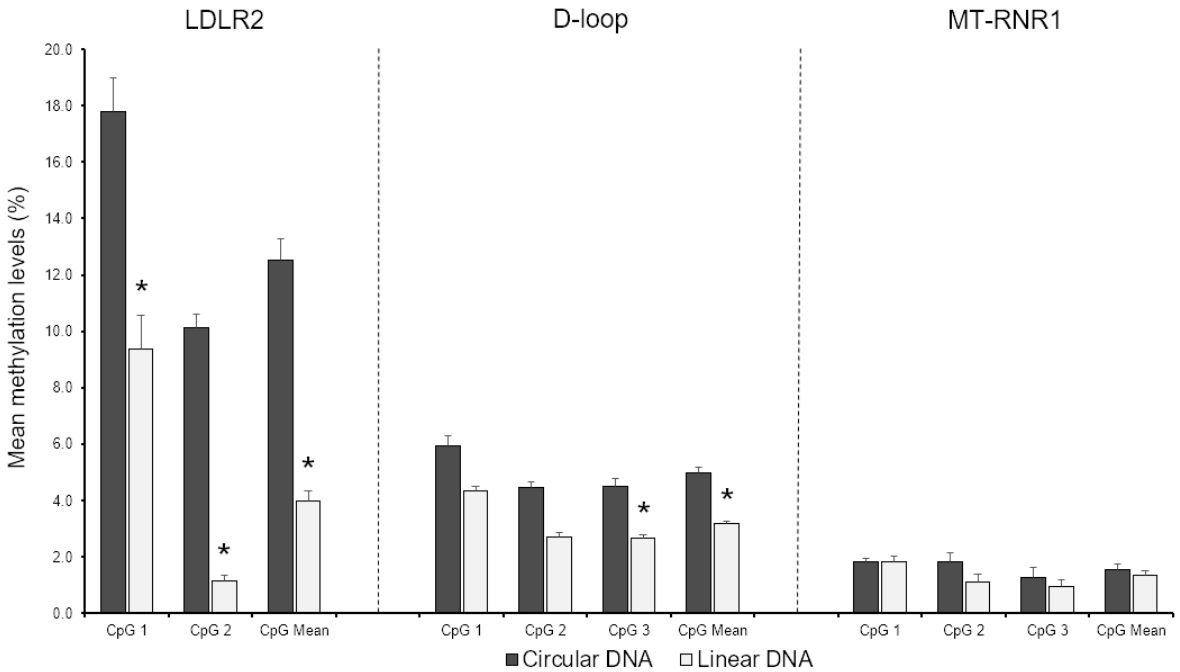

Figure 2: Comparison of methylation levels (%) between linearized and non-linearized mtDNA regions (LDLR2, D-loop, MT-RNR1) in placenta tissue. *Linear mtDNA was obtained using a BamHI restriction enzyme-based treatment. Bar height is equivalent to average methylation levels (LDLR2, D-loop: n = 4; MT-RNR1: n = 5). Error bars represent the standard error of the mean. Asterisks (*) indicate significant differences between linearized and non-linearized mtDNA (Student's t-test, $p < 0.05$).*

A significant difference in mean placental mitochondrial DNA content was observed between the ”Smokers” group compared with the “Control” group with both the relative quantification methods (**Figure 3**). Using the *ND1/RPLP0* ratio to quantify relative mtDNA content, we observed that mothers who smoked during the pregnancy had 0.57 less relative placental mitochondrial DNA content in the on average as compared with the “Control” group, which amounts to a 57.5% decrease. When using the *hmito3/HBB* ratio, the effect size was smaller: 0.44 less relative mitochondrial DNA content was observed in the placenta of mothers that smoked during the pregnancy, which amounts to a 32.6% decrease. Although we observed a declining trend, no significant differences between placental mtDNA content of the “Air Pollution” group compared with the “Control” group were found with either of the quantification methods. Overall, the obtained relative quantities were lower for the *hmito3/HBB* method as compared with the *ND1/RPLP0* method (**Figure 4**).When comparing the results from the two methods, only four of the data points fell outside the limits of agreement as observed in the Bland-Altman plot (**Figure 5**).

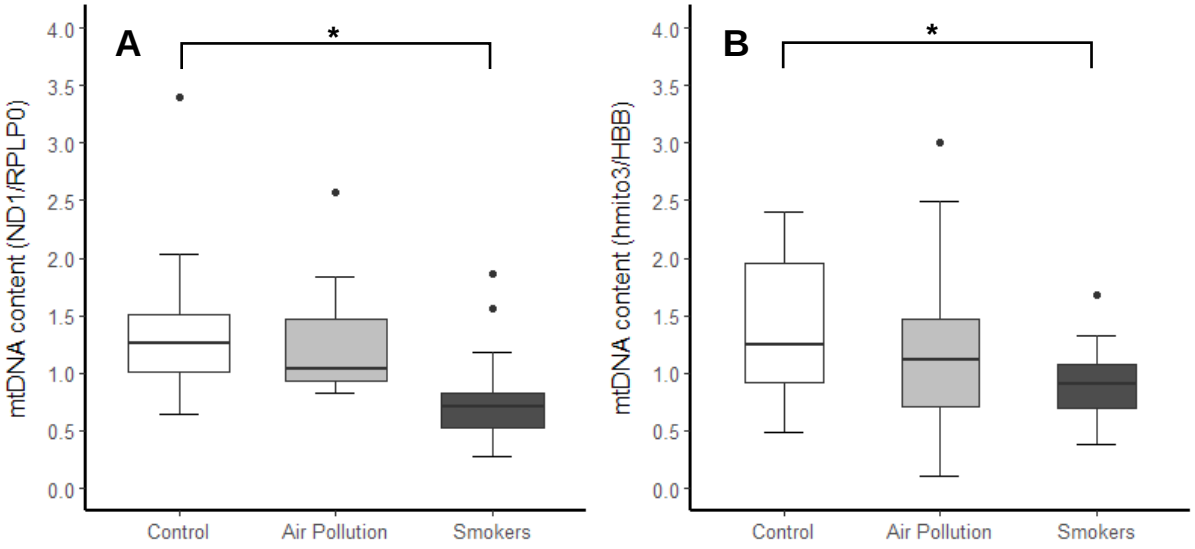

Figure 3: Relative mitochondrial DNA content as determined by RT-qPCR using (A): the ND1 / RPLP0 ratio and (B): the hmito3 / HBB ratio (n = 20 / group). *The solid horizontal line is equivalent to the median. Lower and upper hinges represent to the first and third quartiles (the 25th and 75th percentiles). The upper whisker extends from the hinge to the largest value no further than 1.5 * IQR (= interquartile range) from the hinge, whereas the lower whisker extends from the hinge to the smallest value at most 1.5 * IQR of the hinge. Data outside this range are represented as dots. Asterisks (*) represent significant differences between the exposed groups and the “Control” group at a 95% confidence level (p < 0.05, Dunnett’s test).*

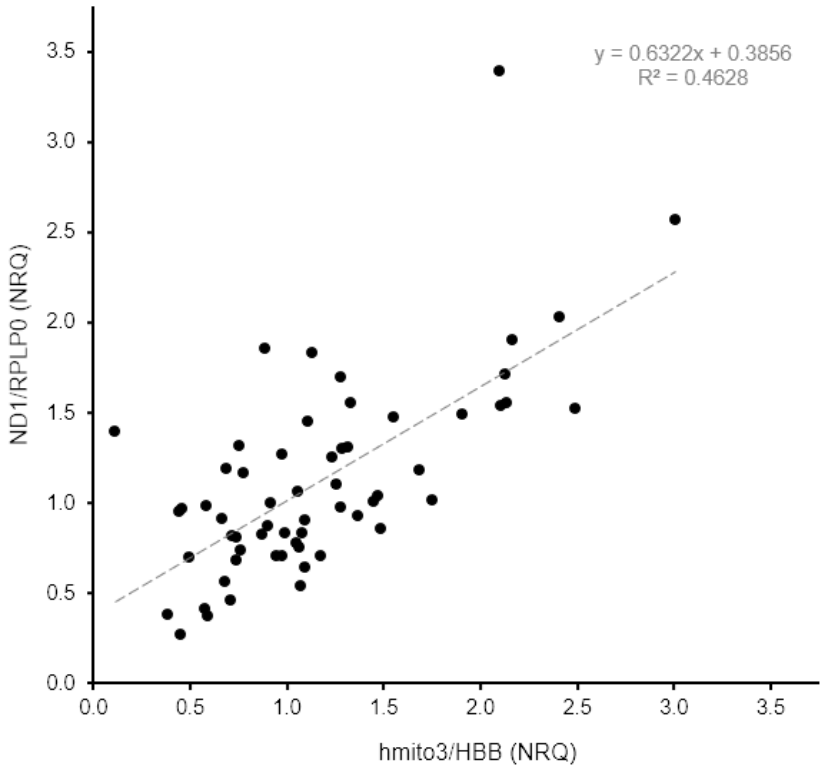

Figure 4: Correlation plot displaying the NRQ values of the ND1/RPLP0 versus the hmito3/HBB mtDNA content assays. *Abbreviations: NRQ: normalized relative quantities.*

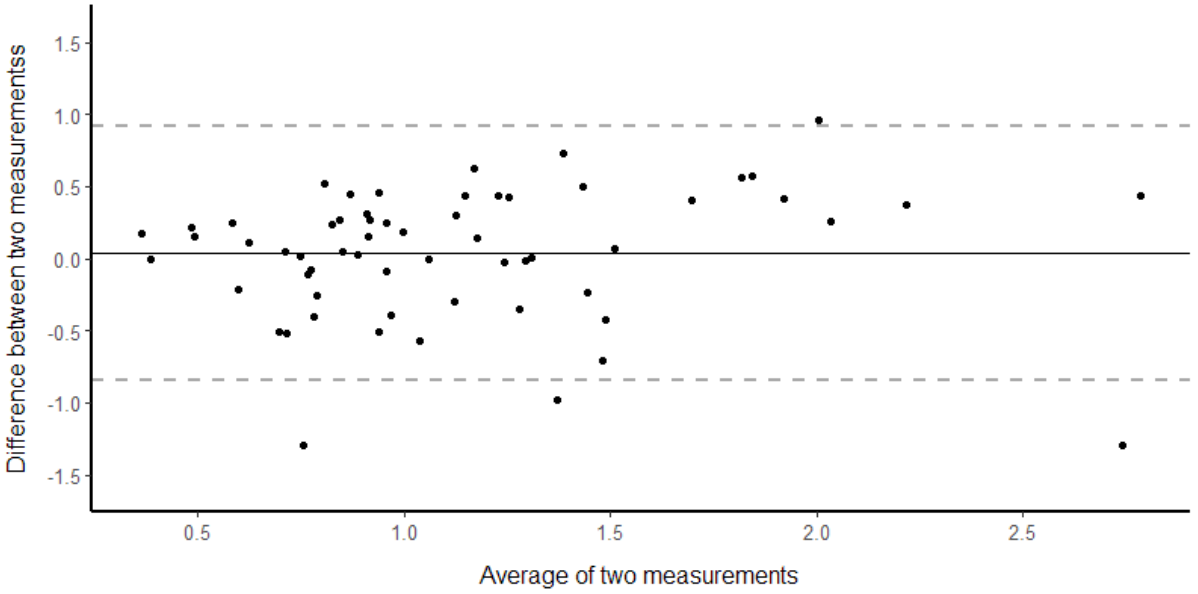

Figure 5: Bland-Altman plot of the measures obtained by the two mitochondrial DNA content assays. *The solid line represents the mean difference between two paired measurements. The dashed lines represent the limits of agreement, which is the confidence interval around the mean difference between two paired measurements at a 95% confidence level.*

In general, methylation levels of the investigated genes were low (ranging from 0% to 5%) for most genes except for *POLG1 exon 2* and *LDLR2*. When analysing the methylation values without adjusting for study population characteristics (**Figure 5**), we observed a significant increase in absolute DNA methylation in the *D-loop* region for the "Air Pollution" group (+0.44%, $p < 0.01$) and the "Smokers" group (+0.36%, $p < 0.01$) as compared with the "Control" group. The other mtDNA region, *LDLR2,* also showed elevated mtDNA methylation levels in both groups, but this trend not significant. For the *PINK1* gene, an opposite effect was found: mean *PINK1* methylation levels in the placenta were lower for both mothers that were highly exposed to air pollution (-0.40%, $p < 0.01$) and for mothers that smoked during the pregnancy (-0.30%, $p = 0.014$) as compared with mothers from the "Control" group.

When analysing the methylation levels using linear mixed effect models and adjusting for population characteristics (maternal education status, parity and pre-gestational BMI, the newborn's gestational age and ethnicity as well as date of delivery), a significant association was found between *in utero* environmental exposures and methylation levels on the *D-loop* region of the mitochondrial DNA (**Table 4**). *D-loop* methylation levels were higher in both exposure groups as compared with the control group ($\beta = +0.61\%$, 95% CI: 0.19 to 1.02 for the "Air Pollution" group, $\beta = +0.40\%$, 95% CI: 0.07 to 0.73 for the "Smokers" group). When adjusting the models for inter-run variation by including the Pyrosequencing Disc ID as a random effect in the model instead of correcting methylation values using an inter-run calibration factor, neither the estimates nor the significance of this finding changed dramatically ($\beta = +0.57\%$, $p < 0.01$ for the "Air Pollution" group, $\beta = +0.39\%$, $p = 0.02$ for the "Smokers" group). A similar trend was observed for *LDLR2* but was not significant ($\beta = +0.77\%$, CI: -0.59 to 2.85). Furthermore, mothers that were highly exposed to air pollution had significantly higher methylation levels on average in the promotor region of the *POLG1* gene ($\beta = +0.77\%$, 95% CI: 0.22 to 1.33) while no effect was observed in the smoker group. When adjusting the model for inter-run variation instead of using corrected methylation values, this finding remained consistent ($\beta = +0.77\%$, $p < 0.01$). No differences between the exposure groups were found for methylation on the second exon of *POLG1*, although overall methylation levels (ranging between 70% and 90%) were much higher than on the *POLG1* promotor region.

A significant interaction was observed between exposure group and methylation on specific CpG sites of the genes *DNA2* and *PINK1*. The post-hoc analysis revealed significant differences between the "Air Pollution" and "Control" group on the third CpG of the *DNA2* target region ($\beta = 1.42$, 95% CI: 0.06 to -2.79), whereas a significant difference was found between the "Smokers" and the "Control" group on the second CpG of the *PINK1* target region ($\beta = 0.76$, 95% CI: 0.16 to 1.37). A borderline significant interaction effect was also observed in the "Air Pollution" model on the *LDLR2* region of the mitochondrial DNA ($p = 0.09$). However, the post-hoc analysis revealed no significant effects on either of the two CpG sites.

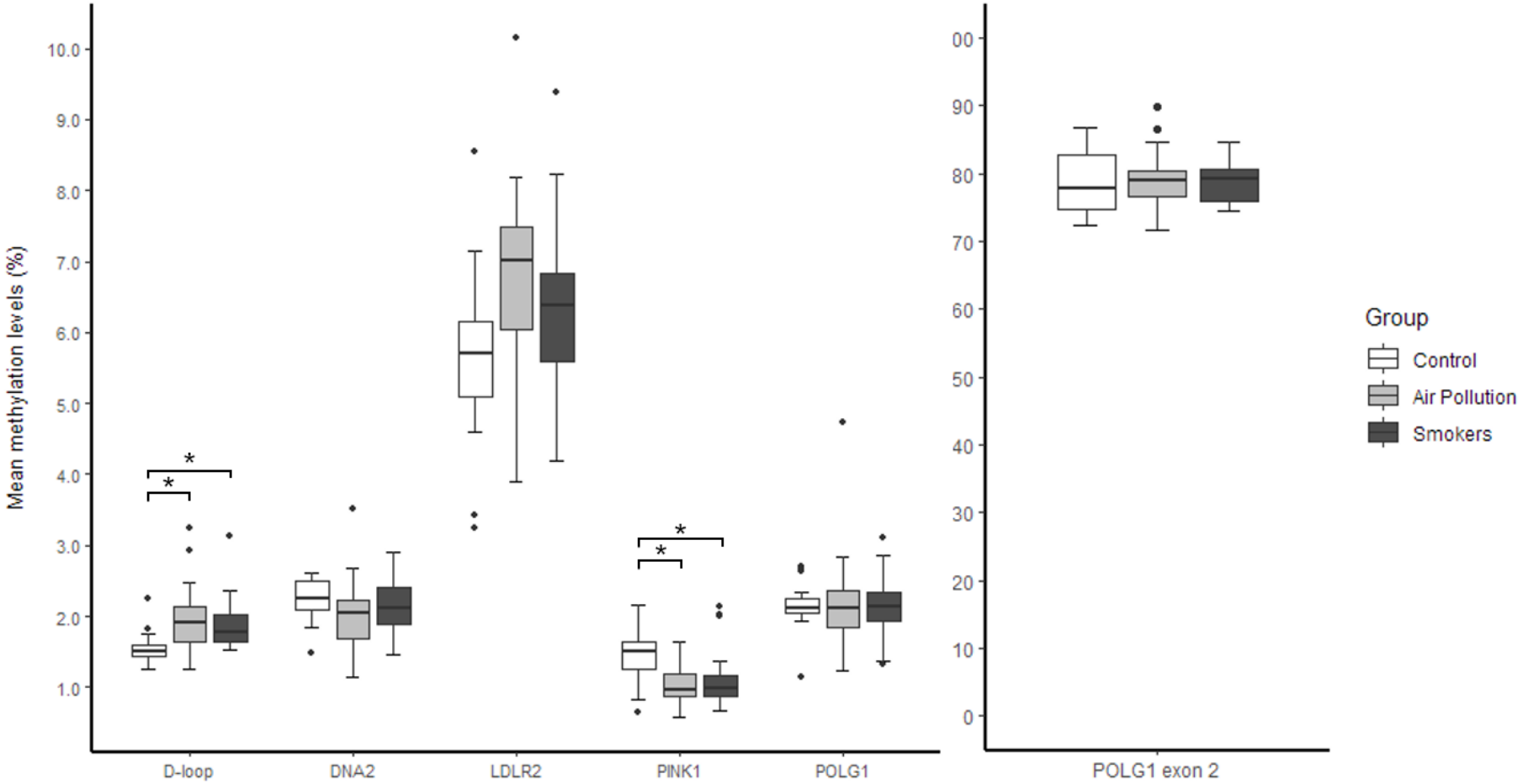

Figure 5: Mean DNA methylation levels as determined by bisulfite pyrosequencing (n = 20 / group). *The solid horizontal line is equivalent to the median. The lower and upper hinges represent the first and third quartiles (the 25th and 75th percentiles). The upper whisker extends from the hinge to the largest value no further than 1.5 * IQR (= interquartile range) from the hinge, whereas the lower whisker extends from the hinge to the smallest value no further than 1.5 * IQR of the hinge. Data outside this range are represented as dots. Asterisks (*) represent significant differences between the groups at a 95% confidence level (p < 0.05) as determined by one-way ANOVA followed by Dunnett's test. All methylation values were corrected for inter-run differences.*

Table 4: Estimates (β) and 95% confidence intervals (CI) for the associations between exposure group and observed methylation levels, as determined by linear mixed models. *All models were adjusted for maternal education, parity, pre-gestational BMI, the newborn's gestational age and ethnicity as well as for the date of delivery. Statistically significant and borderline significant interactions were further examined by one-way ANOVA to determine significant differences between the groups at individual CpG sites. Asterisks represent significant interaction effects at a 95% confidence level (*: p < 0.05, **: p < 0.01) whereas crosses represent borderline significant interaction effects (†: p < 0.10). Statistically significant estimates at a 95% confidence level are highlighted in bold and italic font.*

DNA region	**Control**	**Air Pollution**				**Smokers**			
	Mean	*β (%)*	*Lower CI (%)*	*Upper CI (%)*	*p-value interaction*	*β*	*Lower CI (%)*	*Upper CI (%)*	*p-value interaction*
D-loop	Ref	***0.61***	***0.19***	***1.02***	0.61	***0.40***	***0.07***	***0.73***	0.12
POLG1 (promotor)	Ref	***0.77***	***0.22***	***1.33***	0.30	0.04	- 0.38	0.46	0.18
POLG1 (exon 2)	Ref	1.46	- 3.36	6.29	0.60	1.81	- 2.19	5.81	0.31
LDLR2	Ref	1.13	-0.59	2.85	0.09 (†)	0.17	- 1.19	1.52	0.23
○ CpG 1	Ref	1.02	- 2.26	0.33					
○ CpG 2	Ref	- 0.09	- 0.51	0.33					
DNA2	Ref	0.07	- 0.37	0.52	0.02 (*)	0.16	- 0.07	0.39	0.22
○ CpG 1	Ref	- 0.12	- 0.69	0.45					
○ CpG 2	Ref	0.05	- 0.61	0.71					
○ CpG 3	Ref	***1.42***	***0.06***	***2.79***					
○ CpG 4	Ref	- 0.07	- 0.39	0.25					
○ CpG 5	Ref	0.02	- 0.49	0.52					
○ CpG 6	Ref	- 0.10	- 0.48	0.28					
○ CpG 7	Ref	0.44	- 0.05	0.93					
○ CpG 8	Ref	- 0.29	- 0.65	0.07					
PINK1	Ref	0.31	- 0.07	0.68	< 0.01 (**)	***0.38***	***0.01***	***0.77***	0.03 (*)
○ CpG 1	Ref	0.26	- 0.32	0.83		0.02	- 0.45	0.48	
○ CpG 2	Ref	- 0.18	- 0.77	0.41		0.17	- 0.81	0.47	
○ CpG 3	Ref	0.02	- 0.61	0.65		**0.76**	**0.15**	**1.37**	
○ CpG 4	Ref	- 0.05	- 0.50	0.40		- 0.22	- 0.73	0.29	
○ CpG 5	Ref	0.25	- 0.41	0.91		0.30	- 0.35	0.96	

Using confocal microscopy and a femtosecond pulsed laser-based method to visualise black carbon particles in biological samples, we were able to observe evidence of black carbon particles present in placenta tissue (**Figure 6**). This observation indicates that black carbon particles can translocate from the maternal blood into the placenta tissue despite the presence of the placental barrier.

In addition to the visualisation of black carbon by confocal microscopy, a protocol was tested to determine mitochondrial protein levels (*COX IV*, citrate synthase and *TOM20*) in placenta tissue. Using fluorescent anti-bodies, we were aiming to use a combination of immune-histochemistry and fluorescence confocal microscopy to quantify the proteins of interest. However, we were unable to detect fluorescent any signal with the immunohistochemistry protocols that were used to label the mitochondrial proteins (results not shown).

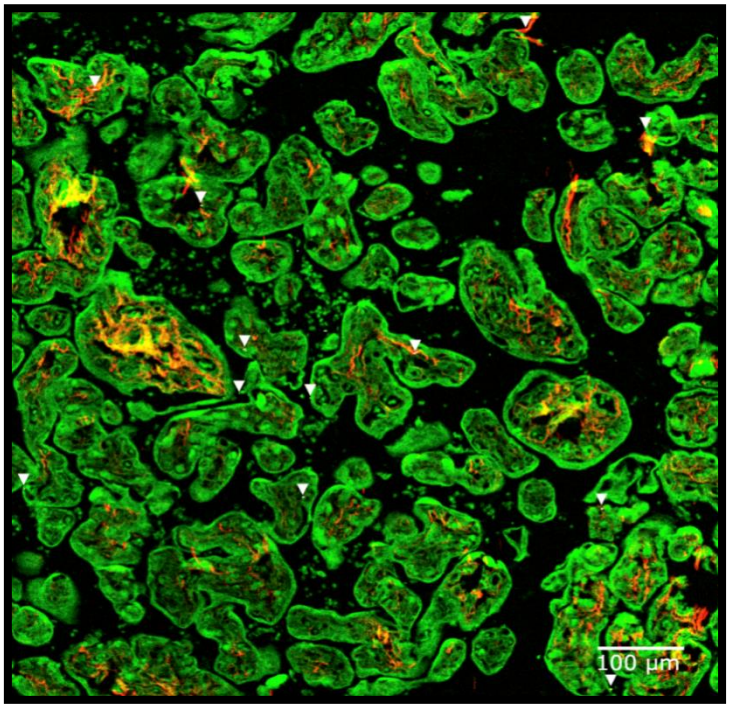

Figure 6: Visualisation of black carbon particles in the placenta. *White light generation originating from the black carbon particles (indicated using white arrowheads) under femtosecond pulsed laser illumination (excitation 810 nm, 80 MHz, 10 mW laser power on the sample) was observed. Second harmonic generation from collagen (red, emission: 400-410 nm) and two-photon autofluorescence (TPAF) from placental and red blood cells (green, emission: 450-650 nm) were simultaneously detected. Scale bar: 100 µm.*

Discussion

Mitochondria are organelles that, through their roles in energy production, regulation of oxidative balance, and cellular signaling are linked with many central processes of cellular function. Given the many roles for mitochondria in cellular homeostasis and regulating pathways, it is natural that the impairment of mitochondrial function can have severe adverse effects.

Deficiencies in placental mitochondrial function can affect the ability of the organ to adequately fulfil the many different roles it plays in foetal development, since mitochondrial energy production is of critical importance throughout the pregnancy (12, 13). *In utero* exposure to environmental pollutants has been associated with several adverse birth outcomes. For example, particulate matter exposure during the pregnancy has been linked with intra-uterine growth restriction (IUGR) (59) and low birthweight (60). In recent years, there has been an increasing number of studies that have investigated the molecular mechanisms behind these associations. However, despite recent investigations, information regarding the potential molecular and functional responses that mitochondria exhibit to prenatal environmental exposures remains scarce. To contribute to this knowledge, this research project aimed to functionally characterize placental mitochondria, while also critically examining key methodological aspects regarding the determination of mitochondrial characteristics.

Mitochondrial DNA structure & observed methylation levels

Previous research regarding methylation on the cytosine residues within the mitochondrial genome has resulted in inconsistent findings. The earliest studies that investigated methylation on the human mitochondrial DNA made use of methyl-sensitive restriction-enzyme based assays to quantify methylation levels, and reported low levels of mtDNA methylation (2 – 5% on CCGG sites) (35, 36). By contrast studies utilizing more modern techniques such as methylated DNA immunoprecipitation (MeDIP) followed by PCR, mass spectrometry and ELISA report higher values, with some reporting methylation levels as high as 13 – 25 % (39). Additionally, studies utilizing bisulfite pyrosequencing to quantify mtDNA methylation have reported relatively higher levels of methylation (42, 43). Yet, other investigations that made use of bisulfite sequencing have reported very low levels of methylation, and present evidence that suggests the absence of biologically relevant levels of mtDNA methylation altogether (45, 47).

Methodological issues regarding the quantification of methylation on mitochondrial DNA likely explain the inconsistencies in literature and have raised doubts about the existence of biologically-relevant cytosine methylation on the mitochondrial genome. Recently published studies demonstrate that the circular structure of mtDNA can lead to incomplete bisulfite conversion, resulting in overestimations of mitochondrial DNA methylation when using quantification methods that require bisulfite treatment (44, 45, 48), such as the pyrosequencing technique that was used in this study. In their investigation into CpG methylation patterns of mitochondrial DNA, Liu *et al.* indicated that the extent to which bisulfite conversion efficiency is affected by mtDNA structure is both region and tissue dependent, a finding

further confirmed by van der Wijst *et al.* (44, 46). Our findings also confirm those results. In placenta tissue, methylation levels in the *LDLR2* and *D-loop* regions were significantly affected by poor bisulfite conversion efficiency on non-linearized mtDNA, although the effect was less pronounced for the *D-loop* region. Methylation levels on the *MT-RNR1* region were not impacted by ineffective bisulfite treatment, with similar methylation values being observed for all treatment conditions. These results indicate that in placenta tissue, the extent to which the mitochondrial DNA is affected by poor bisulfite conversion is highly region dependent, which is consistent with the results from other tissues obtained by both Liu *et al.* and van der Wijst *et al.* (44, 46). Taken together, this indicates that there may be region-specific variances in secondary mtDNA structure across the mitochondrial genome that result in differences regarding bisulfite conversion efficiency. Finally, despite overestimations of mtDNA methylation levels in the past, our results indicate that relevant levels of DNA methylation exist on the mitochondrial genome. Overall methylation levels were relatively low on the D-loop region (ranging between 2% and 6%) and on the *MT-RNR1* region (ranging between 1% and 3.5%). However, on the *LDLR2* region, average methylation levels were higher, particularly on the first CpG site of the target region (~ 10%), which is also consistent with other studies observing similarly high methylation levels on the same CpG site (bp 545) (46). This suggests that while previous studies may have overestimated mtDNA methylation, CpG methylation still exists on specific sites within the mtDNA. This conclusion is further supported by the existence of mitochondria-localized DNA methyltransferase 1 (*mtDNMT1*) enzymes, which have been shown to bind mtDNA and may provide the mechanism by which mtDNA is methylated (37).

There is another important factor that may have contributed to inaccurate assessments of mtDNA methylation levels. Large sections of the mitochondrial genome occur as transcriptionally-inactive pseudogenes on the nuclear DNA. These sequences are also known as nuclear mitochondrial segments (NUMTs) and cover a large portion of the mitochondrial genome (**Figure 7**). In 2015, Janssen *et al.* investigated in placenta tissue the same *MT-RNR1* region that was investigated during this research project (42). They observed much higher methylation levels compared to the values that were observed in this study: average methylation across the two CpGs that were investigated was 9.54%, which is in contrast with the current observation that methylation levels on all three investigated CpGs were below 3%. Since we observed no significant difference between linearized and circular mtDNA, this discrepancy can likely not be attributed to inefficient bisulfite conversion. When using a comparative genomics technique (BLAST) to check the specificity of the PCR amplicon used in the previous study, it was revealed that the amplicon sequence not only occurs on the mitochondrial genome but also on chromosome 7 and chromosome 11 of the nuclear genome. Considering the nuclear DNA is more methylated overall when compared with the mitochondrial DNA, it is likely that the mtDNA methylation values that were determined in the by Janssen *et al.* (2015) were inaccurate due to NUMT contamination. Mechta *et al.* found only a mild correlation between NUMT alignment score and observed methylation levels (45), somewhat contradicting this statement. However, the specificity of our assay is the only variable of note that was changed between this study and the previous assessment of *MT-RNR1* methylation levels by Janssen *et al.* in 2015. Therefore, the findings from this current study stress the need to not only linearize the mitochondrial DNA before bisulfite treatment but also the necessity to

avoid NUMT contamination when designing pyrosequencing assays. However, it should be mentioned that levels of *MT-RNR1* were very low (close to the detection limit), meaning that differences in bisulfite treatment possibly would not have been picked up since methylation levels were close to zero.

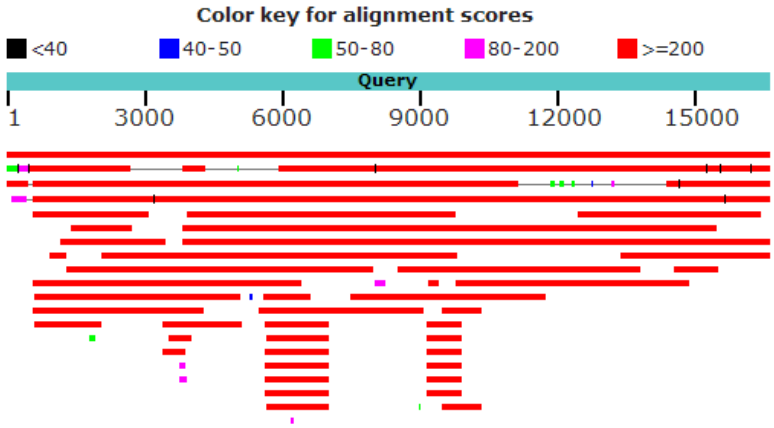

Figure 7: The mitochondrial genome sequence compared against the reference sequence of the human genome using BLAST. *The most matching sequences are shown, with the red bar at the top representing the mitochondrial genome itself (being an exact match), whereas the remaining bars represent regions of the nuclear genome showing a high degree of similarity.*

Environmental exposure & mitochondrial DNA content

Mitochondrial DNA is of critical importance to mitochondrial function and is also especially vulnerable to DNA damage. Because mtDNA repair capacity is less extensive than on the nuclear DNA, mtDNA damage also persists longer (30). Consequently, mitochondrial DNA is an interesting mitochondrial characteristic to investigate in an epidemiological context.

Several research groups have investigated how placental mitochondrial DNA (mtDNA) content is affected under different exposures, and physiological conditions. In 2005, Bouhours-Nouet *et al.* (2005) reported that mothers who smoked during the pregnancy had 37% lower relative mtDNA content in placental tissue than mothers who did not smoke (61), a finding later corroborated by a study from the ENVIR*ON*AGE birth cohort that showed that on average, a group of smokers had 21.6% lower placental mtDNA content compared with a group of non-smokers (62). In this independent study, we observed the same findings. We observed that on average, the “Smokers” group had 57.5% less placental mtDNA content as compared with mothers from the “Control” group. The difference in effect size between these studies may be explained by differences in intensity of tobacco smoke exposure. In our study population, the group of smokers consumed over 13 cigarettes per day during the pregnancy (on average). This in contrast with the study by Janssen *et al.*, where the average number of cigarettes smoked per day during the pregnancy was significantly lower (Janssen *et al.*: over 7 cigarettes/day, Bouhours-Nouet *et al*.: over

10 cigarettes/day), therefore suggesting that the effect *in utero* tobacco smoke exposure on the placental mitochondrial DNA is dose-dependent.

It is worth noting however, that in both umbilical cord serum an opposite relation between tobacco smoke and mtDNA content was found (63). Additionally, a dose dependent association exist between smoking and increased mtDNA content in saliva from human adults (64). While these differences may indicate that the response of mtDNA content to environmental stressors is tissue-specific, there may be methodological issues to consider as well. Notably, the effect size we observed differed depending on the assay used (57.5% for the *ND1/RPLP0* assay versus 32.6% for the *hmito3/HBB* assay). Although neither the significance nor the direction of the effect changed, this difference in effect size is rather large. In a previous study, Malik *et al.* have summarized four major issues that may contribute to inaccurate assessments of mtDNA content and that may explain some of the inconsistencies in literature: [1] the presence of mitochondrial genome segments in the nuclear genome, [2] DNA dilution affecting mitochondrial DNA concentrations differently than nuclear DNA concentrations, [3] inappropriate primer selection and [4] differences in template preparation (65). However, we can seemingly exclude most of these as reasons for the discrepancy between the two assays we tested, as the primers we used are both specific and amplify single-copy genes only. Furthermore, template preparation was the same for both assays. Consequently, the reason for this difference in effect sizes is still uncertain. One explanation could be that the *ND1* assay is not completely specific to the mitochondrial genome, although this is highly unlikely because of the number of mismatches in the forward primer sequence. It is worth noting however, that any combination of these different reasons may explain the differences regarding our study and other studies investigating mtDNA content. More research is needed to more accurately explain these inconsistencies. Methods that quantify mtDNA content in an absolute rather than a relative way, such as digital droplet PCR assays, may provide the information needed to explain these differences in the future. Alternatively, testing both *ND1* and *hmito3* using the same nuclear reference gene may also provide a solution, since any bias stemming from the use of different reference genes can then be excluded.

Despite an association between placental mtDNA content and particulate matter exposure in a previous report (51) we did not observe a significant difference in mtDNA content between the “Air Pollution” and “Control” group although the negative trend was present. Given our limited sample size and the seemingly dose-dependent relation between mtDNA content and environmental exposures, it is not unreasonable to suggest that our current study design simply lacked the statistical power to demonstrate such an association. After all, the effect size expected from air pollution exposure was expected to be smaller as compared with the effect for smoking during the pregnancy, as smoking can be regarded as a high-dosage form of air pollution.

Environmental exposure & DNA methylation

Methylation of cytosine residues on DNA is one of the primary epigenetic mechanisms that influences the regulation of gene expression, with increased methylation levels usually being associated with repressed gene expression. During prenatal development, the epigenome is established in two waves of epigenetic reprogramming: one during early embryogenesis, and one during gametogenesis (66). The relevance of this phenomenon to gene expression regulation and the establishment of cellular identities highlights that epigenetic changes during this time-window can have adverse effects later in life, which is in accordance with the DOHaD hypothesis. Furthermore, evidence indicates that alterations in placental DNA methylation can negatively affect normal fetal and placental development (67).

On the *POLG1* and *PINK1* promotor regions, we observed contrasts between our adjusted and un-adjusted models. In the adjusted model, a significant increase in *PINK1* promotor methylation was found in the "Smokers" when compared to the "Control" group. By contrast, in the unadjusted model, a statistically significant opposite relation was observed for both the "Smokers" and "Air Pollution" groups. Similarly, while the association between *POLG1* methylation and exposure group was not significant in the unadjusted model, it reached significance in the adjusted model. An explanation for this observation may lie in the presence of a confounding variable. Based on our linear mixed effect analysis, date of delivery differed significantly between the exposure groups and was also significantly associated with the observed methylation values for both genes (data not shown). Consequently, the variable may have an important confounding effect on our data, which highlights the need to correct the models for date of delivery. Taken together, our results show a significant positive association between methylation on PINK1 and tobacco smoke exposure and methylation of PINK promotor regions and between the "Air Pollution" group and POLG1 methylation levels.

Additionally, an interesting observation was made regarding the potential epigenetic regulation of *POLG1* gene expression. Overall methylation levels on the second *POLG1* exon were significantly higher as compared with methylation on the promotor region of the gene. This finding is consistent with other studies that have investigated *POLG1 methylation* (68, 69), indicating that this region is likely to be more relevant to the epigenetic regulation of *POLG1* expression than the promotor region. Regardless, we found no significant differences in DNA methylation on *POLG1* exon 2 between any of the exposure groups.

On the mitochondrial genome, significant differences were observed regarding methylation on the *D-loop* region of the mitochondrial genome, with increased methylation levels being observed in both the "Smokers" (+0.40%) and "Air Pollution" (+0.61%) groups as compared with the "Control" group. These findings remained consistent regardless of the analysis method used, giving strong confidence in the validity of the result. Interestingly, the observation is also consistent with the findings from Janssen *et al.* (42), who found that an increase of 3 $\mu g/m^3$ in $PM_{2.5}$ exposure during the entire pregnancy was associated with a 0.21% increase in *D-loop* methylation, despite the previously mentioned overestimations of overall methylation levels in that study. This implies that previous overestimations of mtDNA methylation levels may not necessarily disprove significant associations between environmental

exposures and DNA methylation levels. Nonetheless, results from studies that did not consider bisulfite conversion efficiency should still be interpreted with caution. Additionally, while the association was not significant, we observed an increasing trend in methylation on the *LDLR2* region in both the “Smokers” and “Air Pollution” groups (β. Average methylation levels were higher on the *LDLR2* region (ranging between 4% and 10%) as compared with the *D-loop* region, which is consistent with the results from Breton *et al.* (average methylation of 8.5% for *LDLR2* versus 2.9% for *D-loop*) (70).

Alterations in *D-loop* methylation can affect the replication of the mitochondrial genome, as the mitochondrial origin of replication is located in the *D-loop* region (71). As mentioned above, we observed a significant decrease in mtDNA content for the “Smokers” group, but this was not observed in the “Air Pollution” group despite the difference in *D-loop* methylation being larger (+0.61% versus +0.40%). Nonetheless, previously placental mtDNA content has been associated with air pollution exposure in a relatively large sample size (n = 174) (51). The observed differences in methylation on the *D-loop*, a region highly relevant to mtDNA maintenance and replication, suggest that epigenetic alterations on the mitochondrial genome may explain this association, despite the absence of a significant association between air pollution exposure and mtDNA content in the current study population. Findings from van der Wijst *et al.,* also point in this direction, as they report a correlation between the induction of CpG methylation on the mtDNA and a decrease in mitochondrial DNA copy number in HCT116 cells (46).

An important consideration to make when observing DNA methylation data is the biological relevance of the phenomenon. In this study, we observed low methylation levels in most nuclear genes and, hence, small effect sizes. Only one of the target regions investigated showed relatively high levels of methylation (*POLG1* exon 2, ranging between 70% and 90%), while the methylation in the other regions ranged between 0% and 5%, which raises doubts about the potential regulating effect on gene expression. However, it should be noted that associations between air pollution exposure and small alterations in DNA methylation levels on nuclear DNA genes have been shown previously (33). Additionally, in an epidemiological context, subtle changes in DNA methylation can be meaningful since they can reveal sub-clinical changes that may be at the root of disease development, or hint towards underlying regulating mechanisms. Furthermore, the three genes that were investigated during the current study represent only a small portion of genes that are relevant to mitochondrial function. It is therefore not unreasonable to suggest that despite the current findings, significant associations between air pollution and nuclear gene methylation likely exist for other nuclear genes related to mitochondrial function, including (but not limited to) genes involved in mitochondrial fusion/fission such as OPA1, MFN1 and MFN2 (72).

Lastly, while we observed a significant difference in *D-loop* methylation between the exposure groups, it should be noted that overall methylation levels were low (ranging between 0% and 3.5%). As mentioned above, other studies have questioned the biological relevance of low methylation levels on CpG sites to the regulation of mitochondrial gene expression and mtDNA replication (47). Furthermore, while an association between the induction of high levels of CpG methylation and mitochondrial DNA copy number has been demonstrated in HCT116 cells, there were no effects on mitochondrial gene expression, mitochondrial metabolic activity or mitochondrial superoxide production observed (46). Yet,

despite methylation levels in the *D-loop* region being low, we still observed significant differences between the exposure groups, suggesting that there may yet be a relevant role for mtDNA methylation in the response of the cell to environmental stressors. Therefore, more research into the associations between levels of mtDNA methylation and functional characteristics of mitochondria is needed to firmly conclude on the biological relevance of methylation on the mtDNA, and to clarify its role in the cellular response to environmental stressors and disease.

Conclusions & Synthesis

Mothers that smoked extensively (13 cigarettes/day on average) during the pregnancy had 57.5% less placental mtDNA content as compared with non-smokers. Furthermore, there was a significant association between placental methylation levels on the *D-loop* region of the mitochondrial DNA and tobacco smoke (+0.40%) and air pollution (+0.61%) exposure during the pregnancy. Methylation on the *POLG1* promotor was significantly higher ($\beta = +0.77\%$, $p < 0.01$) in the "Air Pollution" group, whereas *PINK1* methylation was higher in the "Smokers" group ($\beta = +0.76\%$, $p = 0.02$). Additionally, we were able to demonstrate that bisulfite conversion efficiency for placenta tissue is affected by secondary mtDNA structure. Furthermore, our results also indicate that the extent to which bisulfite conversion efficiency is affected by mtDNA structure is very much region-specific. These methodological findings regarding bisulfite sequencing on mitochondrial DNA stress the importance of careful assay design and testing when investigating the mitochondrial genome.

While many of our findings contribute significantly to the current knowledge of mitochondrial characteristics and *in utero* environmental stressors, the current study design still beholds to several key limitations. First and foremost, our sample size was rather limited (n = 20 / group), limiting our ability to detect small differences between the groups. For example, while within the same birth cohort an association between placental mtDNA content and *in utero* exposure to $PM_{2.5}$ was found, we were unable to observe a difference in placental mtDNA content between the "Air Pollution" and "Control" group during this research project. Small differences in methylation levels may also have gone unnoticed because of this limitation. Secondly, while we investigated several key genes, they represent only a small fraction of the total number of genes that are relevant to mitochondrial function. Regarding the mtDNA content determinations, we were not able to identify one clear reason for the discrepancy between the two mtDNA content assays that were tested. Additionally, we only tested one biopt from every placenta, however, previous data from within the research group indicates that within-placenta variation is relatively low for both mtDNA content and DNA methylation measurements (42, 51). Lastly, while mtDNA content and DNA methylation provide useful information regarding mitochondrial integrity, it is ultimately the generation of ATP by the reactions of the ETC that defines mitochondrial function. With the immunohistochemistry staining methods that were used, we were unable to quantify mitochondrial protein levels in the placenta to get a more direct indication of mitochondrial function.

Nonetheless, these limitations simultaneously provide many promising future perspectives to further clarify the current knowledge regarding the influence of *in utero* environmental exposures on mitochondrial function. To get a better understanding of the inconsistencies in mtDNA content determinations, different methodologies that quantify mtDNA content in an absolute instead of a relative way - such as digital droplet PCR – are promising. Alternatively, both RT-PCR assays could be tested using the same nuclear reference gene to exclude any bias that may stem from using different reference genes. Furthermore, to get a more complete picture of relevant epigenetic changes that can impact mitochondrial function, a genome-wide methylation study seems like a promising future direction to take. For example, the SMRT sequencing method by Pacific Biosystems provides a genome-wide approach

to identify not only CpG methylation, but other forms of DNA base modifications as well, without the need for bisulfite conversion. Finally, while we were not able to quantify mitochondrial protein levels, optimization of the protocols that were used are likely to result in methods to perform accurate assessments of mitochondrial protein levels in the placenta. Potential future optimization steps include - but are not limited to - increasing antibody concentrations, using longer deparaffinization phases for the tissue sections and testing different antigen retrieval methods. Another approach to more directly quantify mitochondrial function, would be to determine the enzymatic activities of mitochondrial proteins. However, such assessments require the isolation of intact mitochondria from placenta tissue. Preliminary data from within the research group indicates that such preparations are not trivial, especially from frozen placenta tissue (data not shown). Therefore, the immunohistochemistry staining of mitochondrial protein levels likely represent a more interesting way to more directly assess mitochondrial function.

To conclude, the results obtained during this master thesis project contribute significantly to the current knowledge regarding the health effects of *in utero* environmental exposures, provide future perspectives for continued research and highlight crucial methodological considerations that should be taken into account both when interpreting the results from earlier studies and also when performing new investigations.

References

1. Reece JB, Urry LA, Cain ML, Wasserman SA, Minorsky PV, Jackson RB. Cellular Respiration and Fermentation. Campbell Biology (Global Edition). Ninth ed2012. p. 209-30.
2. Li X, Fang P, Mai J, Choi ET, Wang H, Yang X-f. Targeting mitochondrial reactive oxygen species as novel therapy for inflammatory diseases and cancers. J Hematol Oncol. 2013;6(1):19.
3. Cadenas E, Davies KJ. Mitochondrial free radical generation, oxidative stress, and aging. Free radical biology & medicine. 2000;29(3-4):222-30.
4. Wink DA, Nims RW, Saavedra JE, Utermahlen WE, Ford PC. The Fenton oxidation mechanism: reactivities of biologically relevant substrates with two oxidizing intermediates differ from those predicted for the hydroxyl radical. Proceedings of the National Academy of Sciences. 1994;91(14):6604.
5. Schieber M, Chandel NS. ROS function in redox signaling and oxidative stress. Curr Biol. 2014;24(10):R453-R62.
6. Li X, Fang P, Mai J, Choi ET, Wang H, Yang X-f. Targeting mitochondrial reactive oxygen species as novel therapy for inflammatory diseases and cancers. J Hematol Oncol. 2013;6:19-.
7. Nicholls DG. Mitochondrial function and dysfunction in the cell: its relevance to aging and aging-related disease. The International Journal of Biochemistry & Cell Biology. 2002;34(11):1372-81.
8. Granatiero V, De Stefani D, Rizzuto R. Mitochondrial Calcium Handling in Physiology and Disease. Advances in experimental medicine and biology. 2017;982:25-47.
9. Schapira AH. Mitochondrial diseases. Lancet (London, England). 2012;379(9828):1825-34.
10. Navarro A, Boveris A. Brain mitochondrial dysfunction in aging, neurodegeneration, and Parkinson's disease. Front Aging Neurosci. 2010;2:34.
11. Chen L, Knowlton AA. Mitochondria and heart failure: new insights into an energetic problem. Minerva Cardioangiol. 2010;58(2):213-29.
12. Wakefield SL, Lane M, Mitchell M. Impaired mitochondrial function in the preimplantation embryo perturbs fetal and placental development in the mouse. Biol Reprod. 2011;84(3):572-80.
13. Mayeur S, Lancel S, Theys N, Lukaszewski M-A, Duban-Deweer S, Bastide B, et al. Maternal calorie restriction modulates placental mitochondrial biogenesis and bioenergetic efficiency: putative involvement in fetoplacental growth defects in rats. American Journal of Physiology-Endocrinology and Metabolism. 2012;304(1):E14-E22.
14. Dimauro S, Davidzon G. Mitochondrial DNA and disease. Annals of medicine. 2005;37(3):222-32.
15. Payne BA, Wilson IJ, Yu-Wai-Man P, Coxhead J, Deehan D, Horvath R, et al. Universal heteroplasmy of human mitochondrial DNA. Hum Mol Genet. 2013;22(2):384-90.
16. Martin JL, Brown CE, Matthews-Davis N, Reardon JE. Effects of antiviral nucleoside analogs on human DNA polymerases and mitochondrial DNA synthesis. Antimicrobial agents and chemotherapy. 1994;38(12):2743-9.
17. Arenas-Pinto A, Grant AD, Edwards S, Weller IVD. Lactic acidosis in HIV infected patients: a systematic review of published cases. Sex Transm Infect. 2003;79(4):340-3.
18. Robinson-Papp J, Simpson DM. Neuromuscular diseases associated with HIV-1 infection. Muscle Nerve. 2009;40(6):1043-53.
19. Valko M, Morris H, Cronin MT. Metals, toxicity and oxidative stress. Current medicinal chemistry. 2005;12(10):1161-208.
20. Ott M, Gogvadze V, Orrenius S, Zhivotovsky B. Mitochondria, oxidative stress and cell death. Apoptosis : an international journal on programmed cell death. 2007;12(5):913-22.
21. G. Tyler Miller J, Spoolman SE. Air Pollution. Living in the Environment (International Edition). Seventeenth ed2016. p. 455-62.
22. Tamagawa E, Bai N, Morimoto K, Gray C, Mui T, Yatera K, et al. Particulate matter exposure induces persistent lung inflammation and endothelial dysfunction. Am J Physiol Lung Cell Mol Physiol. 2008;295(1):L79-L85.
23. Pedersen M, Giorgis-Allemand L, Bernard C, Aguilera I, Andersen AM, Ballester F, et al. Ambient air pollution and low birthweight: a European cohort study (ESCAPE). The Lancet Respiratory medicine. 2013;1(9):695-704.
24. Winckelmans E, Cox B, Martens E, Fierens F, Nemery B, Nawrot TS. Fetal growth and maternal exposure to particulate air pollution--More marked effects at lower exposure and modification by gestational duration. Environmental research. 2015;140:611-8.
25. Janssen BG, Madhloum N, Gyselaers W, Bijnens E, Clemente DB, Cox B, et al. Cohort Profile: The ENVIRonmental influence ON early AGEing (ENVIRONAGE): a birth cohort study. International journal of epidemiology. 2017;46(5):1386-7m.
26. Martens DS, Cox B, Janssen BG, Clemente DBP, Gasparrini A, Vanpoucke C, et al. Prenatal Air Pollution and Newborns' Predisposition to Accelerated Biological Aging. JAMA pediatrics. 2017;171(12):1160-7.
27. Manokhina I, Del Gobbo GF, Konwar C, Wilson SL, Robinson WP. Review: placental biomarkers for assessing fetal health. Hum Mol Genet. 2017;26(R2):R237-r45.
28. Chinnery PF, Hudson G. Mitochondrial genetics. British medical bulletin. 2013;106:135-59.
29. Druzhyna NM, Wilson GL, LeDoux SP. Mitochondrial DNA repair in aging and disease. Mech Ageing Dev. 2008;129(7-8):383-90.

30. Yakes FM, Van Houten B. Mitochondrial DNA damage is more extensive and persists longer than nuclear DNA damage in human cells following oxidative stress. Proceedings of the National Academy of Sciences of the United States of America. 1997;94(2):514-9.
31. Janssen BG, Godderis L, Pieters N, Poels K, Kicinski M, Cuypers A, et al. Placental DNA hypomethylation in association with particulate air pollution in early life. Part Fibre Toxicol. 2013;10:22.
32. Cai J, Zhao Y, Liu P, Xia B, Zhu Q, Wang X, et al. Exposure to particulate air pollution during early pregnancy is associated with placental DNA methylation. Sci Total Environ. 2017;607-608:1103-8.
33. Alvarado-Cruz I, Sánchez-Guerra M, Hernández-Cadena L, De Vizcaya-Ruiz A, Mugica V, Pelallo-Martínez NA, et al. Increased methylation of repetitive elements and DNA repair genes is associated with higher DNA oxidation in children in an urbanized, industrial environment. Mutation Research/Genetic Toxicology and Environmental Mutagenesis. 2017;813:27-36.
34. Neven KY, Saenen ND, Tarantini L, Janssen BG, Lefebvre W, Vanpoucke C, et al. Placental promoter methylation of DNA repair genes and prenatal exposure to particulate air pollution: an ENVIRONAGE cohort study. The Lancet Planetary health. 2018;2(4):e174-e83.
35. Shmookler Reis RJ, Goldstein S. Mitochondrial DNA in mortal and immortal human cells. Genome number, integrity, and methylation. The Journal of biological chemistry. 1983;258(15):9078-85.
36. Pollack Y, Kasir J, Shemer R, Metzger S, Szyf M. Methylation pattern of mouse mitochondrial DNA. Nucleic acids research. 1984;12(12):4811-24.
37. Shock LS, Thakkar PV, Peterson EJ, Moran RG, Taylor SM. DNA methyltransferase 1, cytosine methylation, and cytosine hydroxymethylation in mammalian mitochondria. Proceedings of the National Academy of Sciences of the United States of America. 2011;108(9):3630-5.
38. Jia Y, Li R, Cong R, Yang X, Sun Q, Parvizi N, et al. Maternal low-protein diet affects epigenetic regulation of hepatic mitochondrial DNA transcription in a sex-specific manner in newborn piglets associated with GR binding to its promoter. PloS one. 2013;8(5):e63855.
39. Infantino V, Castegna A, Iacobazzi F, Spera I, Scala I, Andria G, et al. Impairment of methyl cycle affects mitochondrial methyl availability and glutathione level in Down's syndrome. Molecular Genetics and Metabolism. 2011;102(3):378-82.
40. Dzitoyeva S, Chen H, Manev H. Effect of aging on 5-hydroxymethylcytosine in brain mitochondria. Neurobiology of Aging. 2012;33(12):2881-91.
41. Byun H-M, Panni T, Motta V, Hou L, Nordio F, Apostoli P, et al. Effects of airborne pollutants on mitochondrial DNA Methylation. Particle and Fibre Toxicology. 2013;10(1):18.
42. Janssen BG, Byun HM, Gyselaers W, Lefebvre W, Baccarelli AA, Nawrot TS. Placental mitochondrial methylation and exposure to airborne particulate matter in the early life environment: An ENVIRONAGE birth cohort study. Epigenetics. 2015;10(6):536-44.
43. Bellizzi D, D'Aquila P, Scafone T, Giordano M, Riso V, Riccio A, et al. The control region of mitochondrial DNA shows an unusual CpG and non-CpG methylation pattern. DNA research : an international journal for rapid publication of reports on genes and genomes. 2013;20(6):537-47.
44. Liu B, Du Q, Chen L, Fu G, Li S, Fu L, et al. CpG methylation patterns of human mitochondrial DNA. Sci Rep. 2016;6:23421.
45. Mechta M, Ingerslev LR, Fabre O, Picard M, Barrès R. Evidence Suggesting Absence of Mitochondrial DNA Methylation. Frontiers in genetics. 2017;8:166-.
46. van der Wijst MG, van Tilburg AY, Ruiters MH, Rots MG. Experimental mitochondria-targeted DNA methylation identifies GpC methylation, not CpG methylation, as potential regulator of mitochondrial gene expression. Sci Rep. 2017;7(1):177.
47. Hong EE, Okitsu CY, Smith AD, Hsieh CL. Regionally specific and genome-wide analyses conclusively demonstrate the absence of CpG methylation in human mitochondrial DNA. Mol Cell Biol. 2013;33(14):2683-90.
48. Owa C, Poulin M, Yan L, Shioda T. Technical adequacy of bisulfite sequencing and pyrosequencing for detection of mitochondrial DNA methylation: Sources and avoidance of false-positive detection. PloS one. 2018;13(2):e0192722.
49. Yakubovskaya E, Chen Z, Carrodeguas JA, Kisker C, Bogenhagen DF. Functional human mitochondrial DNA polymerase gamma forms a heterotrimer. The Journal of biological chemistry. 2006;281(1):374-82.
50. Deas E, Plun-Favreau H, Wood NW. PINK1 function in health and disease. EMBO Mol Med. 2009;1(3):152-65.
51. Janssen BG, Munters E, Pieters N, Smeets K, Cox B, Cuypers A, et al. Placental mitochondrial DNA content and particulate air pollution during in utero life. Environmental health perspectives. 2012;120(9):1346-52.
52. Janssen BG, Gyselaers W, Byun H-M, Roels HA, Cuypers A, Baccarelli AA, et al. Placental mitochondrial DNA and CYP1A1 gene methylation as molecular signatures for tobacco smoke exposure in pregnant women and the relevance for birth weight. Journal of translational medicine. 2017;15(1):5.
53. Alexeyev M, Shokolenko I, Wilson G, LeDoux S. The maintenance of mitochondrial DNA integrity--critical analysis and update. Cold Spring Harbor perspectives in biology. 2013;5(5):a012641.
54. Janssen S, Dumont G, Fierens F, Mensink C. Spatial interpolation of air pollution measurements using CORINE land cover data. Atmospheric Environment. 2008;42(20):4884-903.
55. Lefebvre W, Degrawe B, Beckx C, Vanhulsel M, Kochan B, Bellemans T, et al. Presentation and evaluation of an integrated model chain to respond to traffic- and health-related policy questions. Environmental Modelling & Software. 2013;40:160-70.
56. Malik AN, Czajka A, Cunningham P. Accurate quantification of mouse mitochondrial DNA without co-amplification of nuclear mitochondrial insertion sequences. Mitochondrion. 2016;29:59-64.

57. Bates D, Mächler M, Bolker B, Walker S. Fitting Linear Mixed-Effects Models Using lme4. Journal of Statistical Software; Vol 1, Issue 1 (2015). 2015.
58. Kuznetsova A, Brockhoff PB, Christensen RHB. lmerTest Package: Tests in Linear Mixed Effects Models. Journal of Statistical Software; Vol 1, Issue 13 (2017). 2017.
59. Dejmek J, Selevan SG, Benes I, Solansky I, Sram RJ. Fetal growth and maternal exposure to particulate matter during pregnancy. Environ Health Perspect. 1999;107(6):475-80.
60. Balakrishnan K, Ghosh S, Thangavel G, Sambandam S, Mukhopadhyay K, Puttaswamy N, et al. Exposures to fine particulate matter (PM2.5) and birthweight in a rural-urban, mother-child cohort in Tamil Nadu, India. Environmental research. 2018;161:524-31.
61. Bouhours-Nouet N, May-Panloup P, Coutant R, de Casson FB, Descamps P, Douay O, et al. Maternal smoking is associated with mitochondrial DNA depletion and respiratory chain complex III deficiency in placenta. American journal of physiology Endocrinology and metabolism. 2005;288(1):E171-7.
62. Janssen BG, Gyselaers W, Byun HM, Roels HA, Cuypers A, Baccarelli AA, et al. Placental mitochondrial DNA and CYP1A1 gene methylation as molecular signatures for tobacco smoke exposure in pregnant women and the relevance for birth weight. Journal of translational medicine. 2017;15(1):5.
63. Pirini F, Goldman LR, Soudry E, Halden RU, Witter F, Sidransky D, et al. Prenatal exposure to tobacco smoke leads to increased mitochondrial DNA content in umbilical cord serum associated to reduced gestational age. International journal of environmental health research. 2017;27(1):52-67.
64. Masayesva BG, Mambo E, Taylor RJ, Goloubeva OG, Zhou S, Cohen Y, et al. Mitochondrial DNA content increase in response to cigarette smoking. Cancer epidemiology, biomarkers & prevention : a publication of the American Association for Cancer Research, cosponsored by the American Society of Preventive Oncology. 2006;15(1):19-24.
65. Malik AN, Czajka A. Is mitochondrial DNA content a potential biomarker of mitochondrial dysfunction? Mitochondrion. 2013;13(5):481-92.
66. Messerschmidt DM, Knowles BB, Solter D. DNA methylation dynamics during epigenetic reprogramming in the germline and preimplantation embryos. Genes Dev. 2014;28(8):812-28.
67. Bourque DK, Avila L, Penaherrera M, von Dadelszen P, Robinson WP. Decreased placental methylation at the H19/IGF2 imprinting control region is associated with normotensive intrauterine growth restriction but not preeclampsia. Placenta. 2010;31(3):197-202.
68. Kelly RD, Mahmud A, McKenzie M, Trounce IA, St John JC. Mitochondrial DNA copy number is regulated in a tissue specific manner by DNA methylation of the nuclear-encoded DNA polymerase gamma A. Nucleic acids research. 2012;40(20):10124-38.
69. Steffann J, Pouliet A, Adjal H, Bole C, Fourrage C, Martinovic J, et al. No correlation between mtDNA amount and methylation levels at the CpG island of POLG exon 2 in wild-type and mutant human differentiated cells. Journal of medical genetics. 2017;54(5):324-9.
70. Breton CV, Song AY, Xiao J, Kim S-J, Mehta HH, Wan J, et al. Effects of air pollution on mitochondrial function, mitochondrial DNA methylation, and mitochondrial peptide expression. Mitochondrion. 2019;46:22-9.
71. Fish J, Raule N, Attardi G. Discovery of a major D-loop replication origin reveals two modes of human mtDNA synthesis. Science. 2004;306(5704):2098-101.
72. Scott I, Youle RJ. Mitochondrial fission and fusion. Essays in biochemistry. 2010;47:85-98.

Supplemental information

Supplementary Table 1: Overview of the pyrosequencing assays used. Asterisks (*) indicate the biotinylated primers. *Abbreviations: F: forward primer. R: Reverse primer. S: Sequencing primer. CV: Coefficient of variation.*

Target Region	F/R	Sequence (5' – 3')	Genome location (UCSC, Gr18/hg38)	Amplicon size (bp)
ND1	F	ATGGCCAACCTCCTACTCCT	chrM:3313-3332	115
	R	AAAGGCCCCAACGTTGTAG	chrM:3409-3427	
hmito3	F	CACTTTCCACACAGACATCA	chrM:262-281	129
	R	CCCTAACACCAGCCTAACCA	chrM:369-388	
RPLP0	F	CCCAATTGTCCCCTTACCTT	chr12:120,199,101-120,199,120	85
	R	GAACACAAAGCCCACATTCC	chr12:120,199,166-120,199,185	
HBB	F	GTGCACCTGACTCCTGAGGAGA	chr11:5,226,997-5,227,018	101
	R	CCTTGATACCAACCTGCCCAG	chr11:5,226,917-5,226,937	

Supplementary Table 2: Overview of the pyrosequencing assays used. *Asterisks (*) indicate the biotinylated primers. Abbreviations: F: forward primer. R: Reverse primer. S: Sequencing primer. CV: Coefficient of variation.*

Target region	F/R/S	Bisulfite sequence (5'-3')	Original sequence (5'-3')	Genome location (UCSC, Gr18/hg38)	Amplicon size (bp)	Annealing T (°C)	CpGs (#)
LDLR2	F	TTTTTAGTGTATTGTTTTGAGGAGGTAAGT	TTTTCAGTGTATTGCTTTGAGGAGGTAAGC	chrM:586-615	153	58.7	2
	R (*)	CACTCCCATACTACTAATCTCATCA	TGATGAGATTAGTAGTATGGGAGTG	chrM:463-487			
	S	TGTGTGTGTGTTGGG	TGTGTGTGTGCTGGG	chrM:502-517			
D-loop	F	TGGAAAGTGGTTGTGTAGATATTTAA	TGGAAAGTGGCTGTGCAGAC	chrM:251-270	139	57.4	3
	R (*)	CTTTAATTCCTACCTCATCCTATTATTT	AAATAATAGGATGAGGCAGGAATCAAAG	chrM:132-159			
	S	AATTAATTAATATATTTTAGTAAG	AATTAATTAACACACTTTAGTAAG	chrM:194-217			
MT-RNR1	F	GTAGTTTTTTGGGGTAGAAAA	GTAGTTTTCTGGGGTAGAAAA	chrM:1368-1388	435	57.4	/
(Round 1)	R (*)	CCCTCCCCAATAAAACTAA	TTAGCTTTATTGGGGAGGG	chrM:954-972			
MT-RNR1	F	GTAGTTTTTTGGGGTAGAAAA	GTAGTTTTCTGGGGTAGAAAA	chrM:1368-1388	205	57.4	3
(Round 2)	R (*)	TCATATCCCTCTAAAAAAACCTATTCT	TCATATCCCTCTAGAGGAGCCTGTTCT	chrM:1,184-1,210			
	S	GTTATTTTATGGGTTATATTTTGAT	GCCACCTCATGGCTACACCTTGAC	chrM:1328-1352			
POLG1	F	AAGGGGGATTTTTGGGTG	AAGGGGGACTTCTGGGTG	chr15:89,334,923-89,334,940	215	58.7	3
(Promotor)	R (*)	AACCTACAATCTTCTAATCC	GGATCAGAAGATTGCAGGTT	chr15:89,335,108-89,335,127			
	S	AAGGAGTAGGTGGAT	AAGGAGCAGGTGGAT	chr15:89,334,988-89,335,002			
POLG1	F	AGGTTTTGTTTTTGGGTTAGGAG	AGGCTCTGCTTCTGGGCCAGGAG	chr15:89,333,312-89,333,334	234	58.7	8
(Exon 2)	R (*)	ACACAACCCATTAAACATCCAAATA	CATCTGGATGTCCAATGGGTTGTGC	chr15:89,333,521-89,333,545			
	S	GGGTAAGGGTACGGTTGGTTGTTTTTA	GGGCAAGGGCACGGCTGGCTGCCCCCA	chr15:89,333,392-89,333,418			
PINK1	F	TGGTGAGGGTTTGGGGTTG	TGGTGCGGGCCTGGGGCTG	chr1:20,633,805-20,633,831	142	58.7	5
	R (*)	ACCCCCCTCACCTAAATCTCCTA	GCCCCGCTCACCTGGATCTCCTGAC	chr1:20,633,922-20,633,946			
	S	TTGGGTTTTATAGAGGAAAAATAG	CTGGGCCTCATCGAGGAAAAACAG	chr1:20,633,870-20,633,893			
DNA2	F	AGAAAGTTTAGAAAAGGGAAAAAGG	AGAAAGCTTAGAAAAGGGAAAAAGG	chr10:68,471,923-68,471,947	198	57.4	8
	R (*)	AAAAACTCCCTATATTCCCAATCC	GAAGACTCCCTGTATTCCCAGTCC	chr10:68,472,097-68,472,120			
	S	AATTAGTAGATGTTTTAAATGATT	AACCCGCAGATGTCCCAAATGACCT	chr10:68,471,979-68,472,003			